

Binary-driven hypernovae and the understanding of long gamma-ray bursts

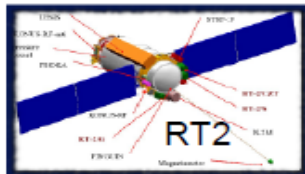
Jorge Armando Rueda Hernández

International Center for Relativistic Astrophysics Network - ICRA-Net
Pescara and Rome

In collaboration with:

Y. Aimuratov, L. Becerra, C. L. Bianco, C. Cherubini, C. L. Ellinger, S. Filippi, C. Fryer, M. Guzzo, M. Karlica,
D. Melon, R. Moradi, D. Primorac, J. F. Rodriguez, F. Rossi-Torres, R. Ruffini, N. Sahakyan, J. D. Uribe, Y.
Wang

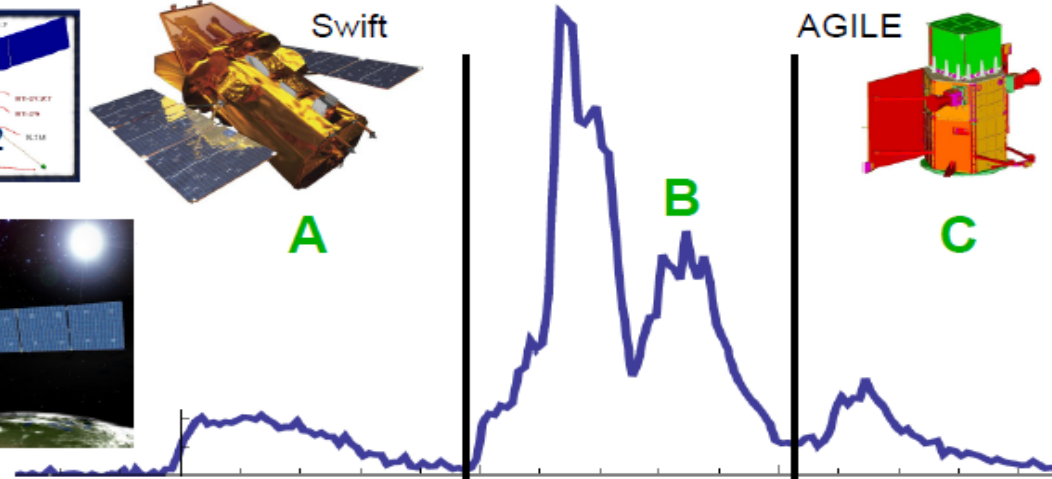
15th Marcel Grossmann Meeting on Relativistic Astrophysics
July 1-7, Rome 2017



A



Ferm



GRB 090618

$$E_{iso} = 2.8 \times 10^{53} \text{ erg}$$

Z=0.54

Ruffini et al. *PoS(Texas 2010)*, 101 (2011)
Izzo et al., *A&A*, 543, A10 (2012)

Faulkes North



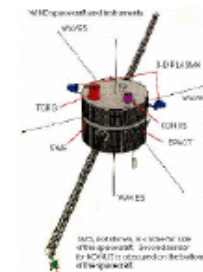
Gemini North



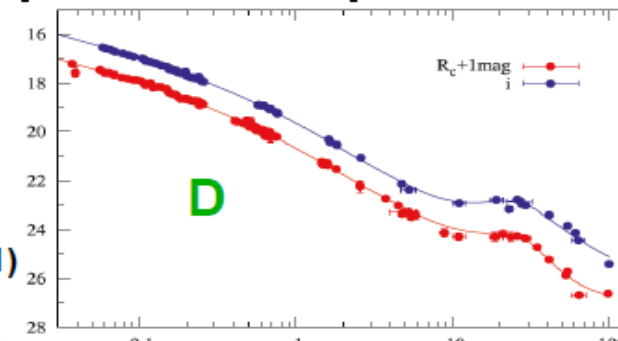
Herschel telescope



¹⁰⁰ Newton telescope



Konus-WIND

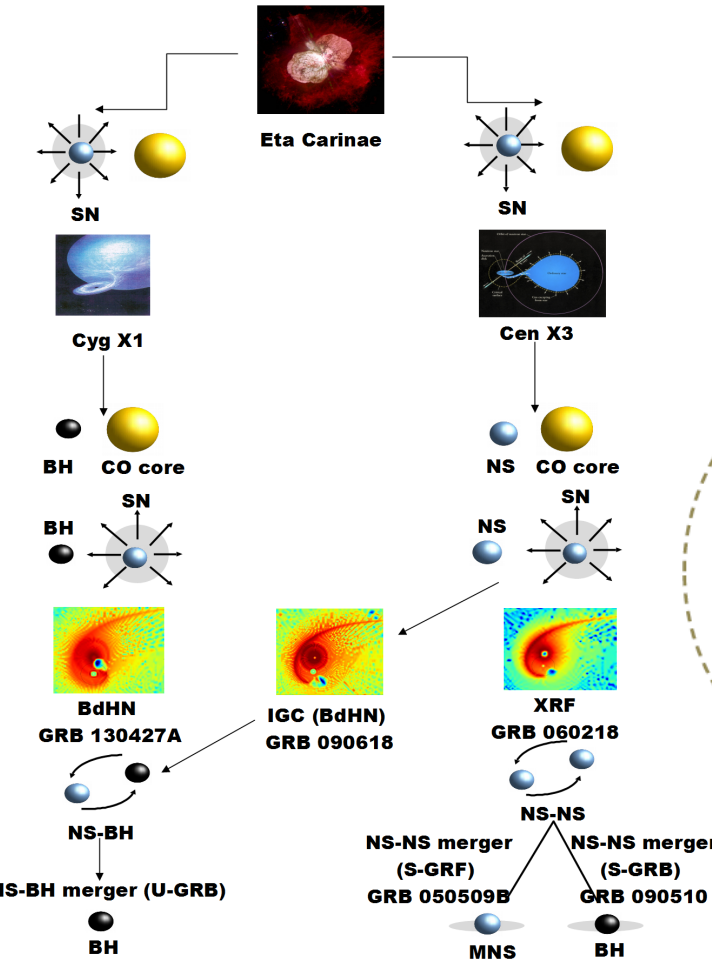


Short and long GRB sub-classes

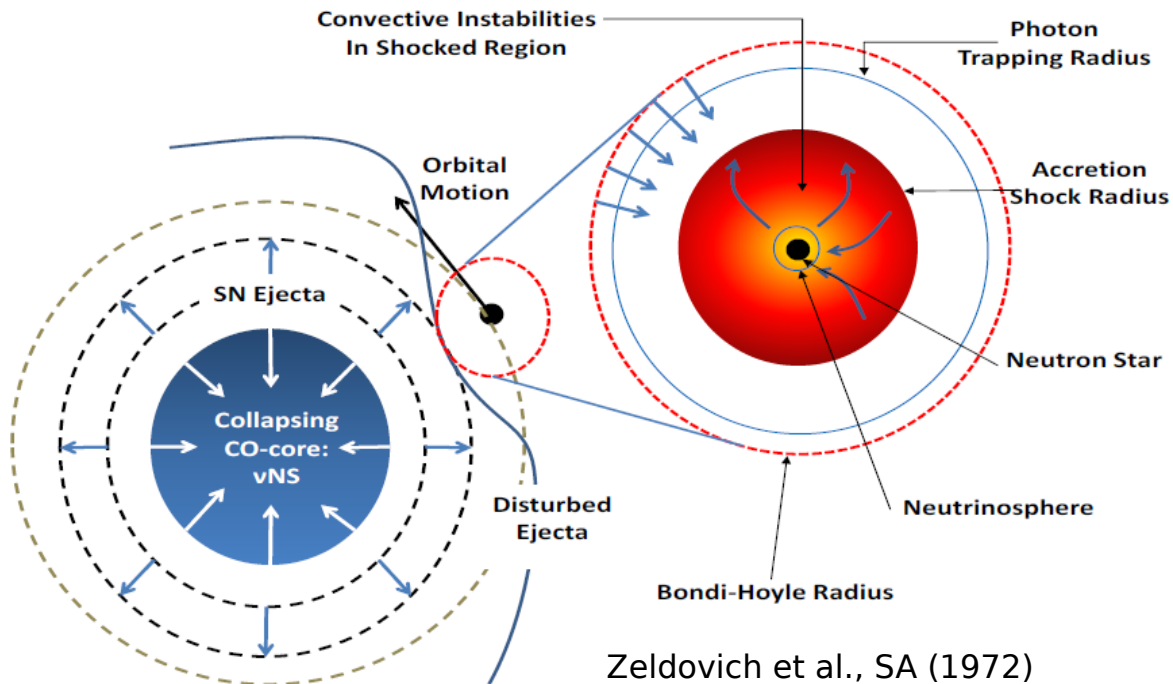
Table 1. Summary of the astrophysical aspects of the different GRB sub-classes and of their observational properties. In the first four columns we indicate the GRB sub-classes and their corresponding *in-states* and the *out-states*. In columns 5–8 we list the ranges of $E_{\text{p},i}$ and E_{iso} (rest-frame 1– 10^4 keV), $E_{\text{iso,X}}$ (rest-frame 0.3–10 keV), and $E_{\text{iso,GeV}}$ (rest-frame 0.1–100 GeV). Columns 9 and 10 list, for each GRB sub-class, the maximum observed redshift and the local observed rate ρ_{GRB} obtained in Ruffini et al. (2016b).

	Sub-class	<i>In-state</i>	<i>Out-state</i>	$E_{\text{p},i}$ (MeV)	E_{iso} (erg)	$E_{\text{iso,X}}$ (erg)	$E_{\text{iso,GeV}}$ (erg)	z_{max}	ρ_{GRB} (Gpc $^{-3}$ yr $^{-1}$)
I	XRFs	CO _{core} -NS	ν NS-NS	$\lesssim 0.2$	$\sim 10^{48}\text{--}10^{52}$	$\sim 10^{48}\text{--}10^{51}$	—	1.096	100^{+45}_{-34}
II	BdHNe	CO _{core} -NS	ν NS-BH	$\sim 0.2\text{--}2$	$\sim 10^{52}\text{--}10^{54}$	$\sim 10^{51}\text{--}10^{52}$	$\lesssim 10^{53}$	9.3	$0.77^{+0.09}_{-0.08}$
III	BH-SN	CO _{core} -BH	ν NS-BH	$\gtrsim 2$	$> 10^{54}$	$\sim 10^{51}\text{--}10^{52}$	$\gtrsim 10^{53}$	9.3	$\lesssim 0.77^{+0.09}_{-0.08}$
IV	S-GRFs	NS-NS	MNS	$\lesssim 2$	$\sim 10^{49}\text{--}10^{52}$	$\sim 10^{49}\text{--}10^{51}$	—	2.609	$3.6^{+1.4}_{-1.0}$
V	S-GRBs	NS-NS	BH	$\gtrsim 2$	$\sim 10^{52}\text{--}10^{53}$	$\lesssim 10^{51}$	$\sim 10^{52}\text{--}10^{53}$	5.52	$(1.9^{+1.8}_{-1.1}) \times 10^{-3}$
VI	U-GRBs	ν NS-BH	BH	$\gtrsim 2$	$> 10^{52}$	—	—	—	$\gtrsim 0.77^{+0.09}_{-0.08}$
VII	GRFs	NS-WD	MNS	$\sim 0.2\text{--}2$	$\sim 10^{51}\text{--}10^{52}$	$\sim 10^{49}\text{--}10^{50}$	—	2.31	$1.02^{+0.71}_{-0.46}$

A common evolutionary scenario for short and long GRBs



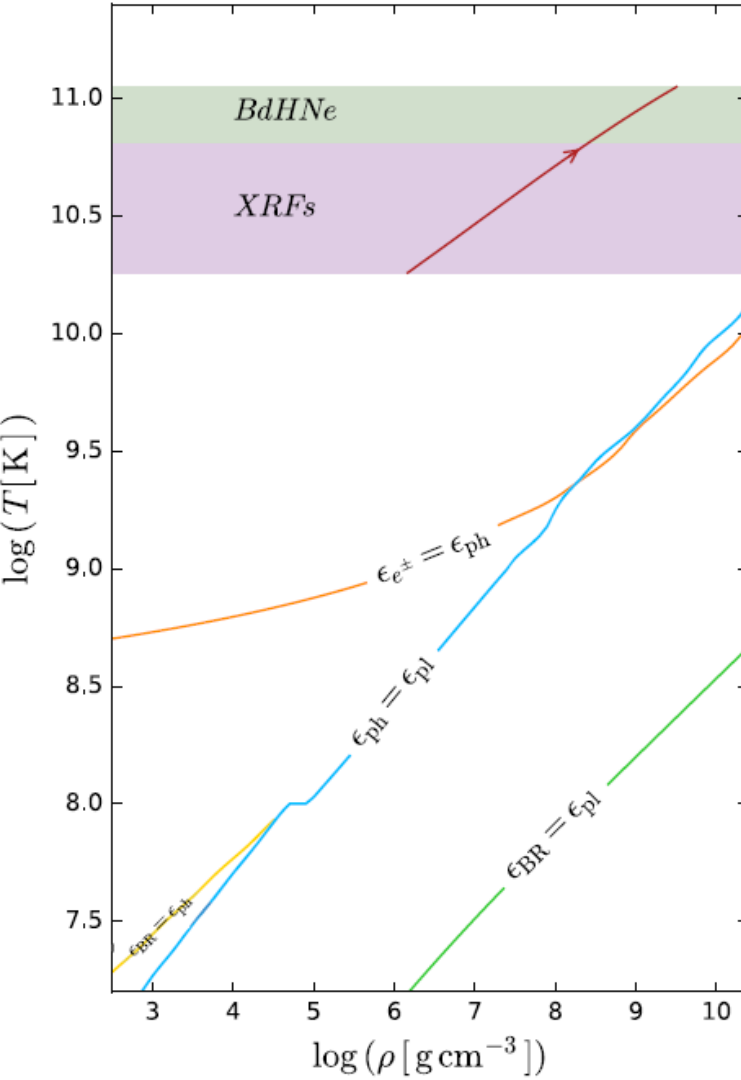
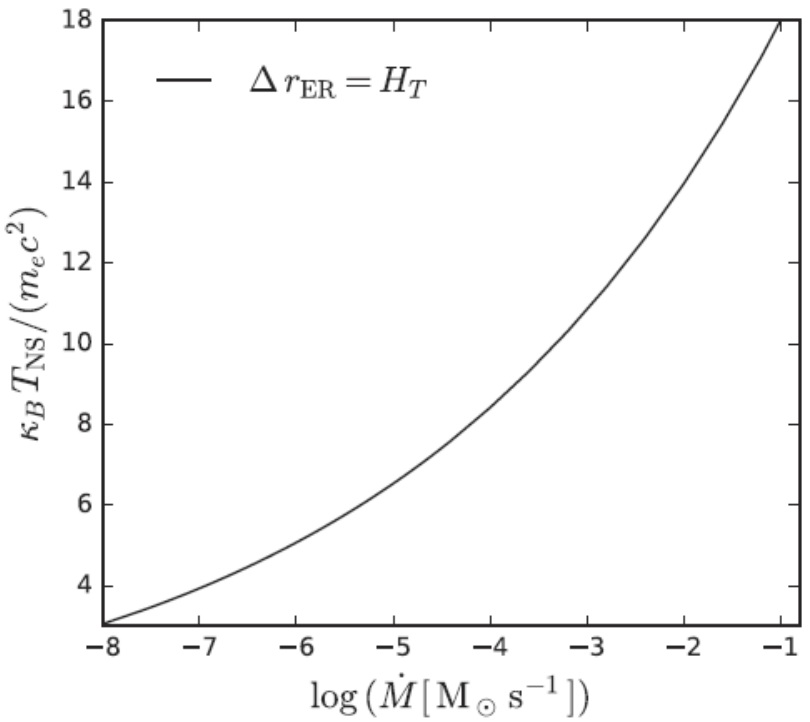
Binary-driven hypernovae (BdHNe)



Zeldovich et al., SA (1972)
 Ruffini & Wilson, PRL (1973)
 Rueda & Ruffini, ApJL (2012)
 Fryer, Rueda, Ruffini, ApJL (2014)

T-rho near the NS surface and neutrino production

Becerra, Bianco, Fryer, Rueda, Ruffini, ApJ 2016;
arXiv:1606.02523



Some numbers related to the neutrino emission

Becerra, Guzzo, Rueda, Ruffini, Uribe, Torres, ApJ 2018; arXiv:1712.07210

\dot{M} ($M_\odot \text{ s}^{-1}$)	ρ (g cm^{-3})	$k_B T$ (MeV)	η_{e^+}	$n_{e^-} - n_{e^+}$ (cm^{-3})	$k_B T_{\nu\bar{\nu}}$ (MeV)	$\langle E_\nu \rangle$ (MeV)	$F_{\nu_e, \bar{\nu}_e}^C$ ($\text{cm}^{-2} \text{s}^{-1}$)	$F_{\nu_x, \bar{\nu}_x}^C$ ($\text{cm}^{-2} \text{s}^{-1}$)	$n_{\nu_e \bar{\nu}_e}^C$ (cm^{-3})	$n_{\nu_x \bar{\nu}_x}^C$ (cm^{-3})	$\sum_i n_{\nu_i \bar{\nu}_i}^C$ (cm^{-3})
10^{-8}	1.46×10^6	1.56	∓ 0.325	4.41×10^{29}	1.78	6.39	4.17×10^{36}	1.79×10^{36}	2.78×10^{26}	1.19×10^{26}	3.97×10^{26}
10^{-7}	3.90×10^6	2.01	∓ 0.251	1.25×10^{30}	2.28	8.24	3.16×10^{37}	1.36×10^{37}	2.11×10^{27}	9.00×10^{26}	3.01×10^{27}
10^{-6}	1.12×10^7	2.59	∓ 0.193	3.38×10^{30}	2.93	10.61	2.40×10^{38}	1.03×10^{38}	1.60×10^{28}	6.90×10^{27}	2.29×10^{28}
10^{-5}	3.10×10^7	3.34	∓ 0.147	9.56×10^{30}	3.78	13.69	1.84×10^{39}	7.87×10^{38}	1.23×10^{29}	5.20×10^{28}	1.75×10^{29}
10^{-4}	8.66×10^7	4.30	∓ 0.111	2.61×10^{31}	4.87	17.62	1.39×10^{40}	5.94×10^{39}	9.24×10^{29}	3.96×10^{29}	1.32×10^{30}
10^{-3}	2.48×10^8	5.54	∓ 0.082	7.65×10^{31}	6.28	22.70	1.04×10^{41}	4.51×10^{40}	7.00×10^{30}	3.00×10^{30}	1.00×10^{31}
10^{-2}	7.54×10^8	7.13	∓ 0.057	2.27×10^{32}	8.08	29.22	7.92×10^{41}	3.39×10^{41}	5.28×10^{31}	2.26×10^{31}	7.54×10^{31}

$$T_{\text{acc}} \approx \left(\frac{3P_{\text{shock}}}{4\sigma/c} \right)^{1/4} = \left(\frac{7}{8} \frac{\dot{M}_{\text{acc}} v_{\text{acc}} c}{4\pi R_{\text{NS}}^2 \sigma} \right)^{1/4}$$

$$\epsilon_{e^- e^+} \approx 8.69 \times 10^{30} \left(\frac{k_B T}{1 \text{ MeV}} \right)^9 \text{ MeV cm}^{-3} \text{ s}^{-1}$$

$$\Delta r_\nu = \frac{\epsilon_{e^- e^+}}{\nabla \epsilon_{e^- e^+}} = \frac{\Delta r_{\text{ER}}}{9} \approx 0.08 R_{\text{NS}}$$

$$L_\nu \approx 4\pi R_{\text{NS}}^2 \Delta r_\nu \epsilon_{e^- e^+} \approx 10^{48} - 10^{57} \text{ MeV s}^{-1}$$

$$n_{\nu_i}^C = n_{\bar{\nu}_i}^C, \quad F_{\nu_i}^C = F_{\bar{\nu}_i}^C \quad \forall i \in \{e, \mu, \tau\}$$

$$\frac{n_{\nu_e}^C}{n_{\nu_x}^C} = \frac{n_{\bar{\nu}_e}^C}{n_{\bar{\nu}_x}^C} = \frac{F_{\nu_e}^C}{F_{\nu_x}^C} = \frac{F_{\bar{\nu}_e}^C}{F_{\bar{\nu}_x}^C} \approx \frac{7}{3}.$$

$$\frac{\varepsilon_e^0}{\varepsilon_x^0} = \frac{\varepsilon_e^0}{\varepsilon_\mu^0 + \varepsilon_\tau^0} = \frac{C_{+,e}^2}{C_{+,\mu}^2 + C_{+,\tau}^2} \approx \frac{7}{3}$$

NS EOS (Relativistic Mean-Field Models)

(e.g. Rueda, Ruffini, Xue, Nucl. Phys. A 872, 286, 2011)

$$\mathcal{L} = \mathcal{L}_g + \mathcal{L}_f + \mathcal{L}_\sigma + \mathcal{L}_\omega + \mathcal{L}_\rho + \mathcal{L}_\gamma + \mathcal{L}_{\text{int}}$$

$$\mathcal{L}_g = -\frac{R}{16\pi G},$$

$$\mathcal{L}_\gamma = -\frac{1}{16\pi} F_{\mu\nu} F^{\mu\nu},$$

$$\mathcal{L}_\sigma = \frac{1}{2} \nabla_\mu \sigma \nabla^\mu \sigma - U(\sigma), \quad U(\sigma) = U_0 + U(\sigma, 4)$$

$$\mathcal{L}_\omega = -\frac{1}{4} \Omega_{\mu\nu} \Omega^{\mu\nu} + \frac{1}{2} m_\omega^2 \omega_\mu \omega^\mu,$$

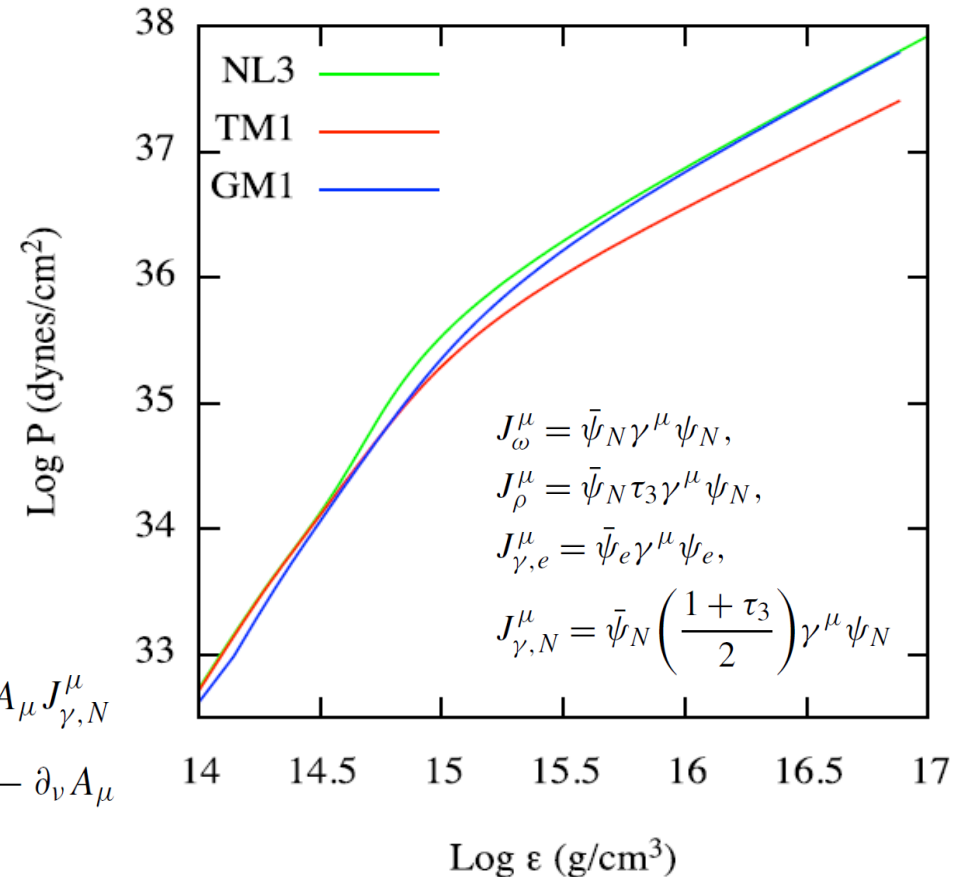
$$\mathcal{L}_\rho = -\frac{1}{4} \mathcal{R}_{\mu\nu} \mathcal{R}^{\mu\nu} + \frac{1}{2} m_\rho^2 \rho_\mu \rho^\mu,$$

$$\mathcal{L}_{\text{int}} = -g_\sigma \sigma \bar{\psi}_N \psi_N - g_\omega \omega_\mu J_\omega^\mu - g_\rho \rho_\mu J_\rho^\mu + e A_\mu J_{\gamma,e}^\mu - e A_\mu J_{\gamma,N}^\mu$$

$$\Omega_{\mu\nu} \equiv \partial_\mu \omega_\nu - \partial_\nu \omega_\mu, \quad \mathcal{R}_{\mu\nu} \equiv \partial_\mu \rho_\nu - \partial_\nu \rho_\mu, \quad F_{\mu\nu} \equiv \partial_\mu A_\nu - \partial_\nu A_\mu$$

$$U_0 \equiv \frac{1}{2} m_\sigma^2 \sigma^2,$$

$$U(\sigma, 4) \equiv \frac{1}{3} g_2 \sigma^3 + \frac{1}{4} g_3 \sigma^4$$



Rotating NSs: full rotation in GR

(e.g. Cipolletta et al., PRD 2015; arXiv: 1506.05926)

$$ds^2 = -e^{2\nu} dt^2 + e^{2\psi} (d\phi - \omega dt)^2 + e^{2\lambda} (dr^2 + r^2 d\theta^2) \quad T^{\alpha\beta} = (\varepsilon + P) u^\alpha u^\beta + Pg^{\alpha\beta}$$

$$\nabla \cdot (B \nabla \nu) = \frac{1}{2} r^2 \sin^2 \theta B^3 e^{-4\nu} \nabla \omega \cdot \nabla \omega + 4\pi B e^{2\zeta-2\nu} \left[\frac{(\varepsilon + P)(1 + v^2)}{1 - v^2} + 2P \right]$$

$$\nabla \cdot (r^2 \sin^2 \theta B^3 e^{-4\nu} \nabla \omega) = -16\pi r \sin \theta B^2 e^{2\zeta-4\nu} \frac{(\varepsilon + P)v}{1 - v^2} \quad \nabla \cdot (r \sin(\theta) \nabla B) = 16\pi r \sin \theta B e^{2\zeta-2\nu} P,$$

$$\begin{aligned} \zeta_{,\mu} = & - \left\{ (1 - \mu^2) \left(1 + r \frac{B_{,r}}{B} \right)^2 + \left[\mu - (1 - \mu^2) \frac{B_{,r}}{B} \right]^2 \right\}^{-1} \left[\frac{1}{2} B^{-1} \left\{ r^2 B_{,rr} - [(1 - \mu^2) B_{,\mu}]_{,\mu} - 2\mu B_{,\mu} \right\} \right. \\ & \times \left\{ -\mu + (1 - \mu^2) \frac{B_{,\mu}}{B} \right\} + r \frac{B_{,r}}{B} \left[\frac{1}{2} \mu + \mu r \frac{B_{,r}}{B} + \frac{1}{2} (1 - \mu^2) \frac{B_{,\mu}}{B} \right] + \frac{3}{2} \frac{B_{,\mu}}{B} \left[-\mu^2 + \mu (1 - \mu^2) \frac{B_{,\mu}}{B} \right] \\ & - (1 - \mu^2) r \frac{B_{,\mu r}}{B} \left(1 + r \frac{B_{,r}}{B} \right) - \mu r^2 (\nu_{,r})^2 - 2 (1 - \mu^2) r \nu_{,\mu} \nu_{,r} + \mu (1 - \mu^2) (\nu_{,\mu})^2 - 2 (1 - \mu^2) r^2 B^{-1} B_{,r} \nu_{,\mu} \nu_{,r} \\ & + (1 - \mu^2) B^{-1} B_{,\mu} \left[r^2 (\nu_{,r})^2 - (1 - \mu^2) (\nu_{,\mu})^2 \right] + (1 - \mu^2) B^2 e^{-4\nu} \left\{ \frac{1}{4} \mu r^4 (\omega_{,r})^2 + \frac{1}{2} (1 - \mu^2) r^3 \omega_{,\mu} \omega_{,r} \right. \\ & \left. - \frac{1}{4} \mu (1 - \mu^2) r^2 (\omega_{,\mu})^2 + \frac{1}{2} (1 - \mu^2) r^4 B^{-1} B_{,r} \omega_{,\mu} \omega_{,r} - \frac{1}{4} (1 - \mu^2) r^2 B^{-1} B_{,\mu} \left[r^2 (\omega_{,r})^2 - (\mu^2) (\omega_{,\mu})^2 \right] \right\} \end{aligned}$$

Neutron Star Binding Energy

(Cipolletta et al., Phys. Rev. D 2015; arXiv: 1506.05926)

Static Configurations

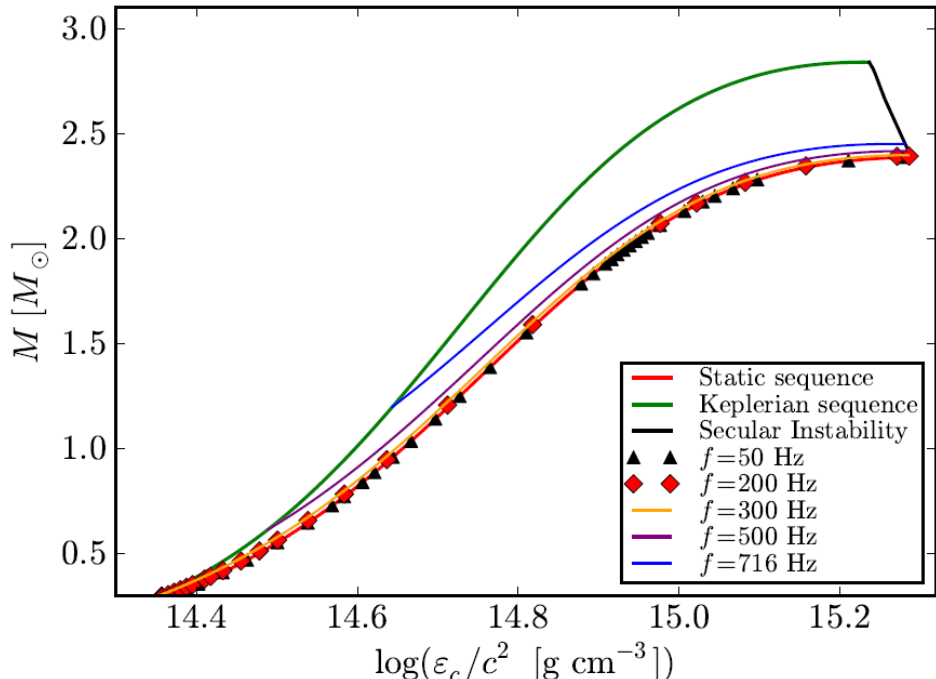
$$\frac{M_b}{M_\odot} \approx \frac{M}{M_\odot} + \frac{13}{200} \left(\frac{M}{M_\odot} \right)^2$$

$c J/(G M_\odot^2)$

Rotating Configurations

$$\frac{M_b}{M_\odot} = \frac{M}{M_\odot} + \frac{13}{200} \left(\frac{M}{M_\odot} \right)^2 \left(1 - \frac{1}{130} j^{1.7} \right)$$

Neutron star stability region



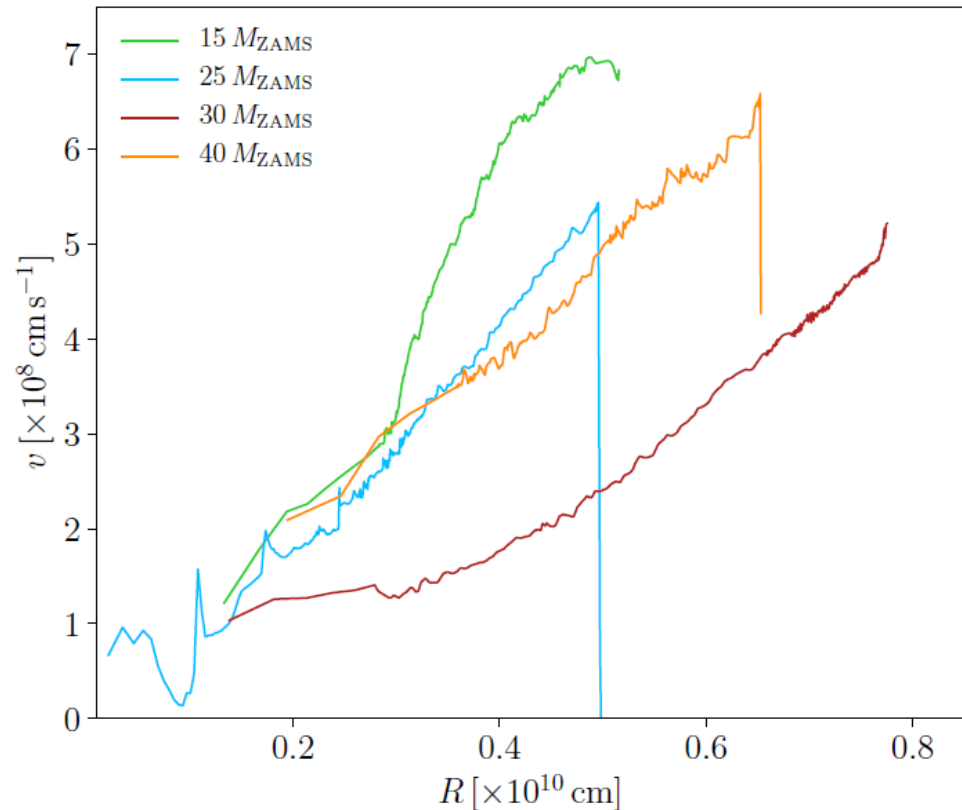
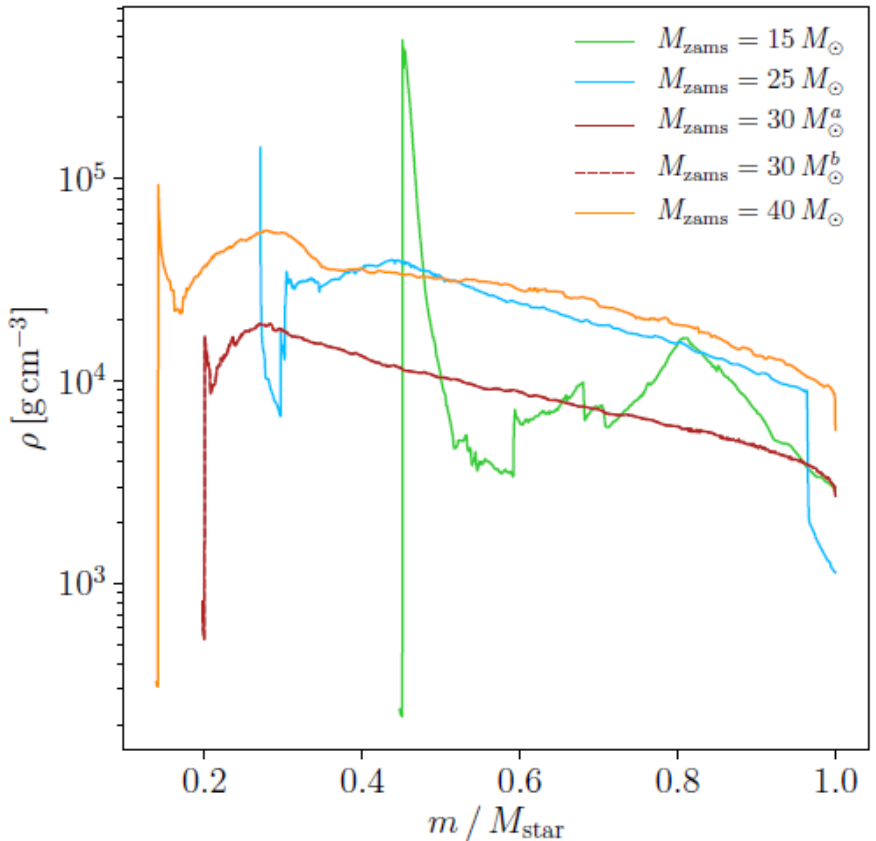
$$M_{\text{NS}}^{\text{crit}} = M_{\text{NS}}^{J=0} (1 + k j_{\text{NS}}^p)$$

	$M_{\text{crit}}^{J=0}$ M_\odot	$R_{\text{crit}}^{J=0}$ km	$M_{\text{max}}^{J \neq 0}$ M_\odot	$R_{\text{max}}^{J \neq 0}$ km	f_K kHz	p	k
NL3	2.81	13.49	3.38	17.35	1.34	1.68	0.006
GM1	2.39	12.56	2.84	16.12	1.49	1.69	0.011
TM1	2.20	12.07	2.62	15.98	1.40	1.61	0.017

Taken from Cipolletta, Cherubini, Filippi, Rueda, Ruffini, PRD (2015); arXiv:1506.05926

First simulations (1D): ICRANet-LANL Collaboration

SN at t=0 (shock at CO-core surface)

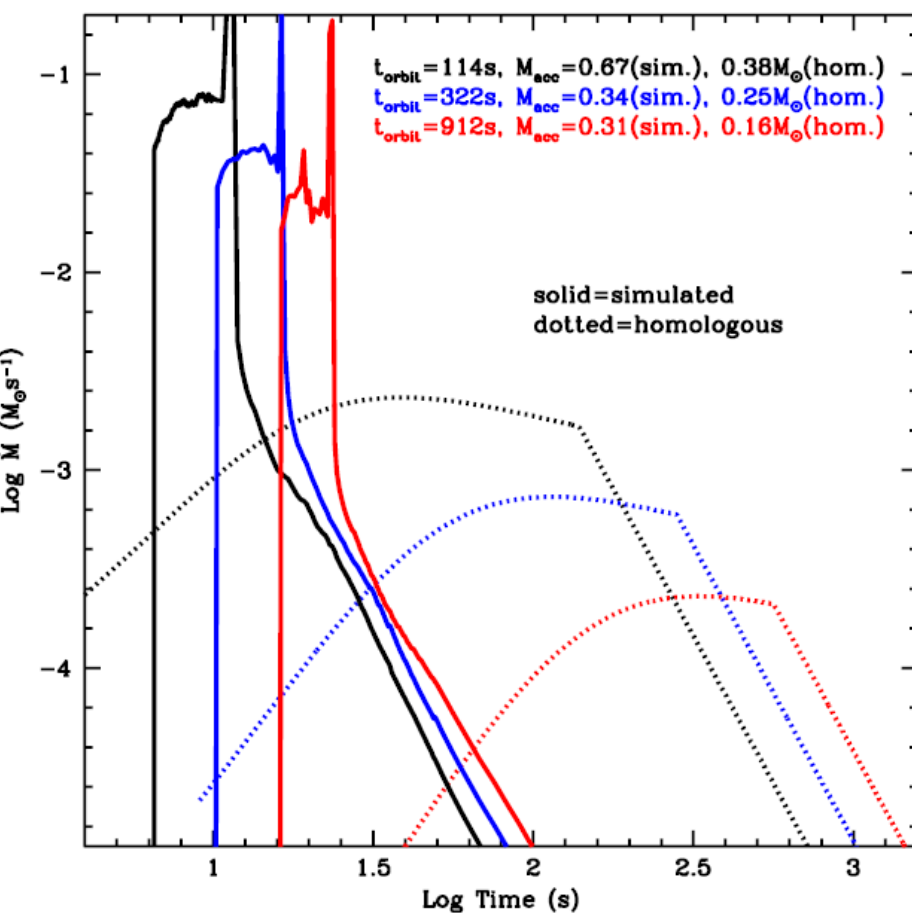
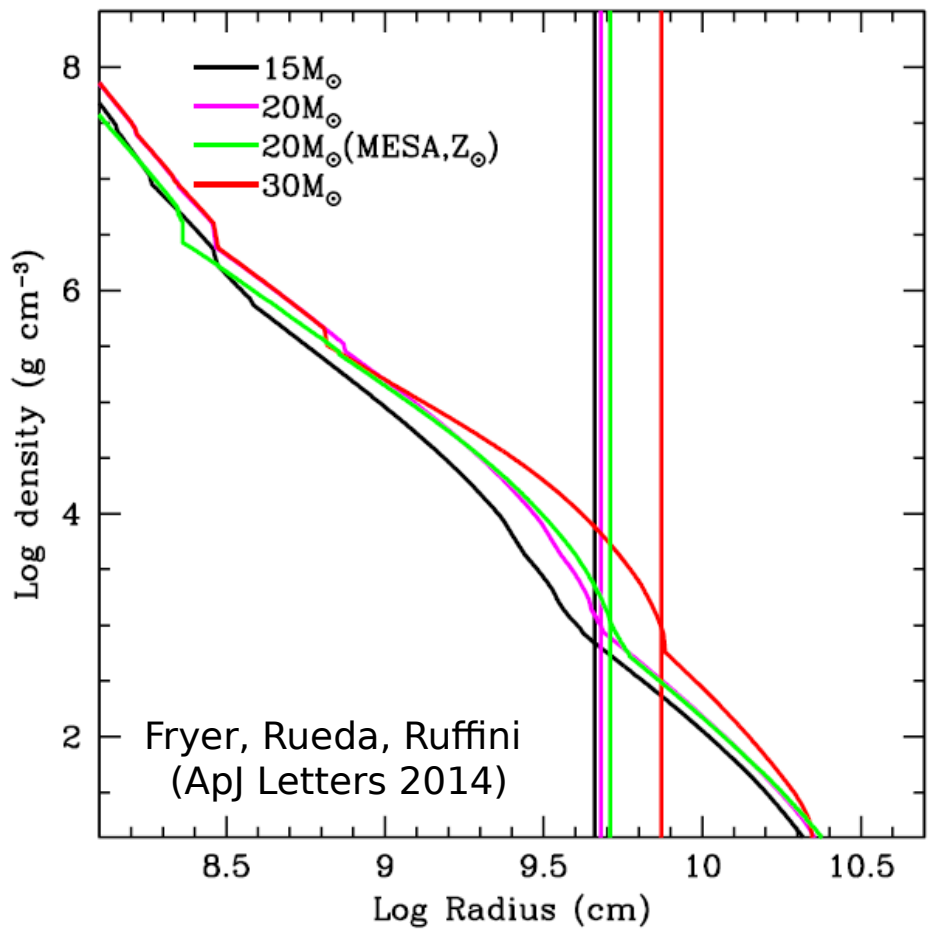


Initial conditions from Los Alamos core-collapse SN code

$$\dot{M}_{\text{BHL}} = 4\pi r_{\text{BHL}}^2 \rho (v^2 + c_s^2)^{1/2}$$

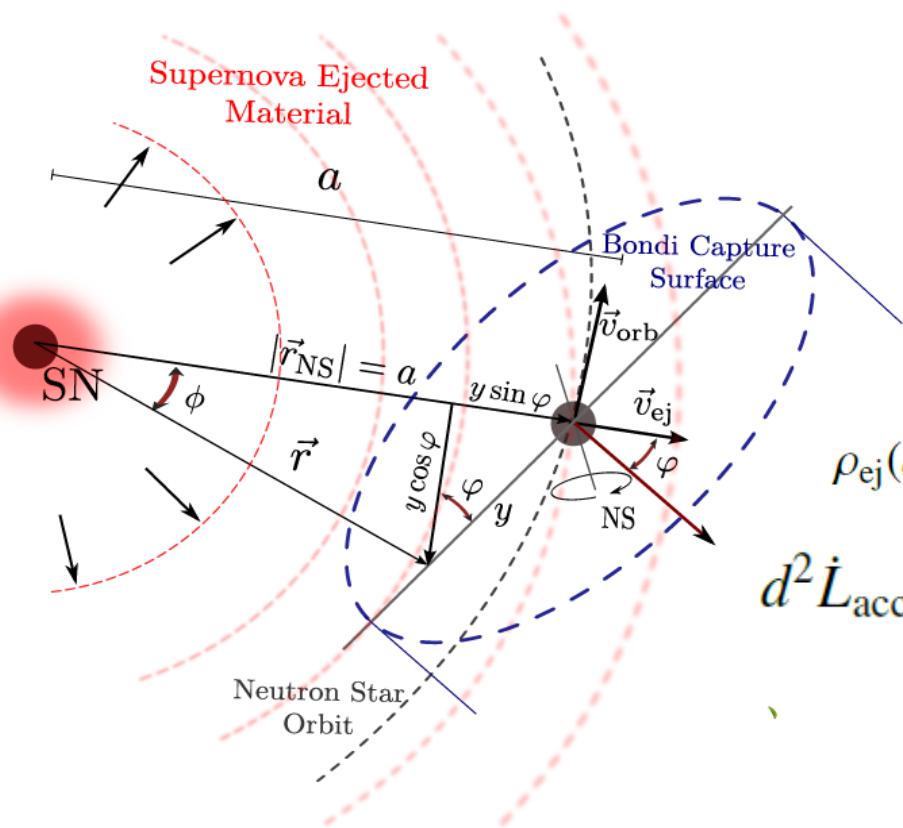
$$r_{\text{BHL}} = \frac{GM_{\text{NS}}}{v^2 + c_s^2}$$

$$r_{\text{trapping}} = \min[(\dot{M}_{\text{BHL}} \kappa) / (4\pi c), r_{\text{BHL}}]$$



Role of angular momentum in BdHNe

(Becerra, Cipolletta, Fryer, Rueda, Ruffini, ApJ 2015; arXiv: 1505.07580)



$$\dot{M}_B(t) = \pi \rho_{\text{ej}} R_{\text{cap}}^2 \sqrt{v_{\text{rel}}^2 + c_{s,\text{ej}}^2}$$

$$R_{\text{cap}}(t) = \frac{2GM_{\text{NS}}(t)}{v_{\text{rel}}^2 + c_{s,\text{ej}}^2}$$

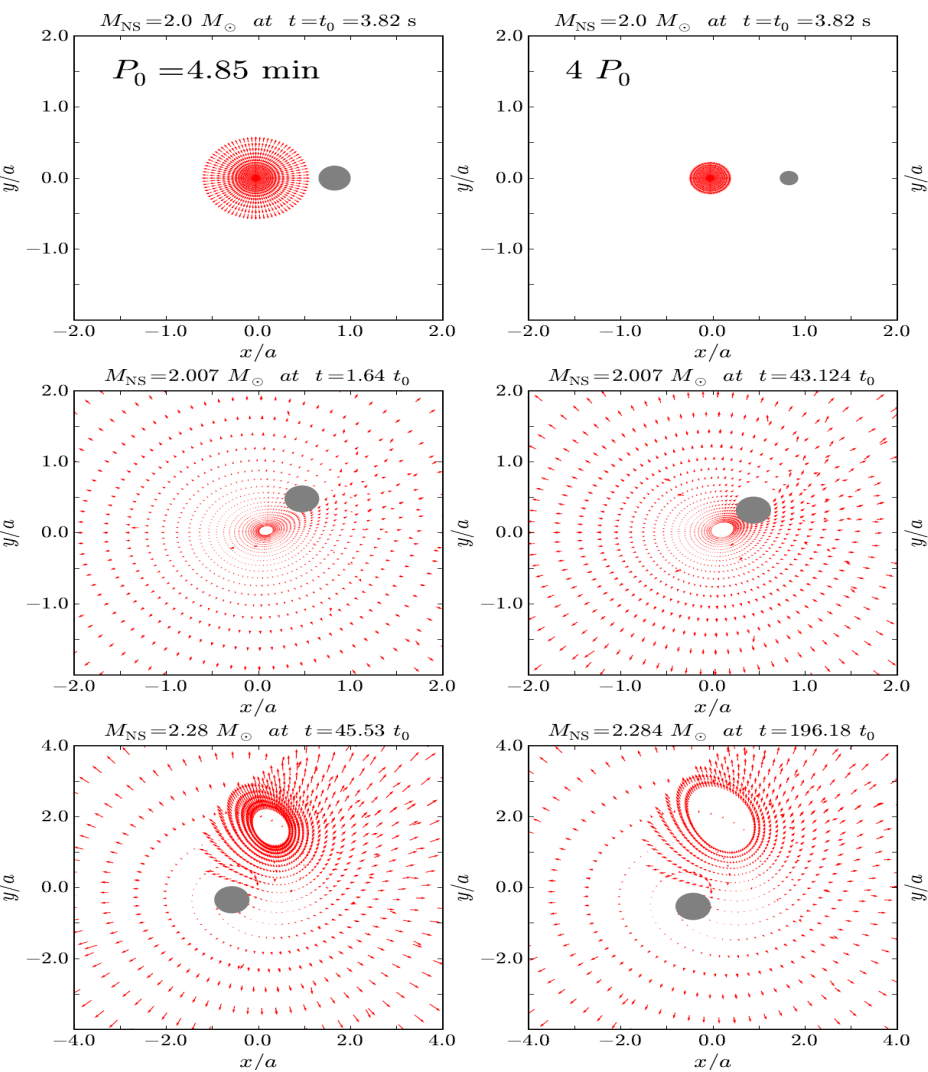
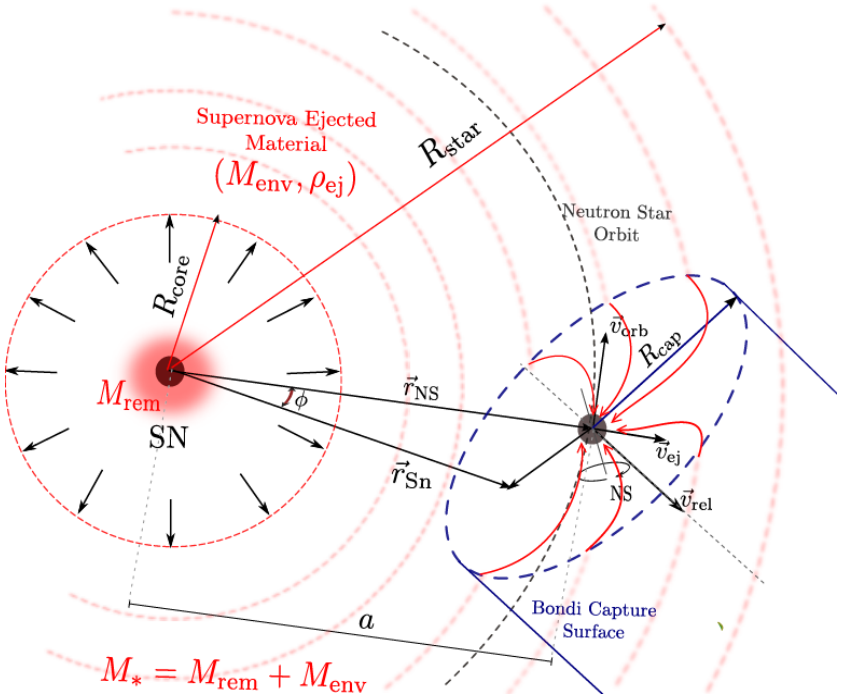
$$\rho_{\text{ej}}(a) \simeq \rho_{\text{ej}}(a)(1 + \epsilon_\rho y) \quad \text{and} \quad v_{\text{rel}}(a) \simeq v_{\text{rel}}(a)(1 + \epsilon_v y)$$

$$d^2 \dot{L}_{\text{acc}} = \rho_{\text{ej}}(a) v_{\text{rel}}^2(a) \left[y + (\epsilon_\rho + 2\epsilon_v)y^2 \right] dy dz$$

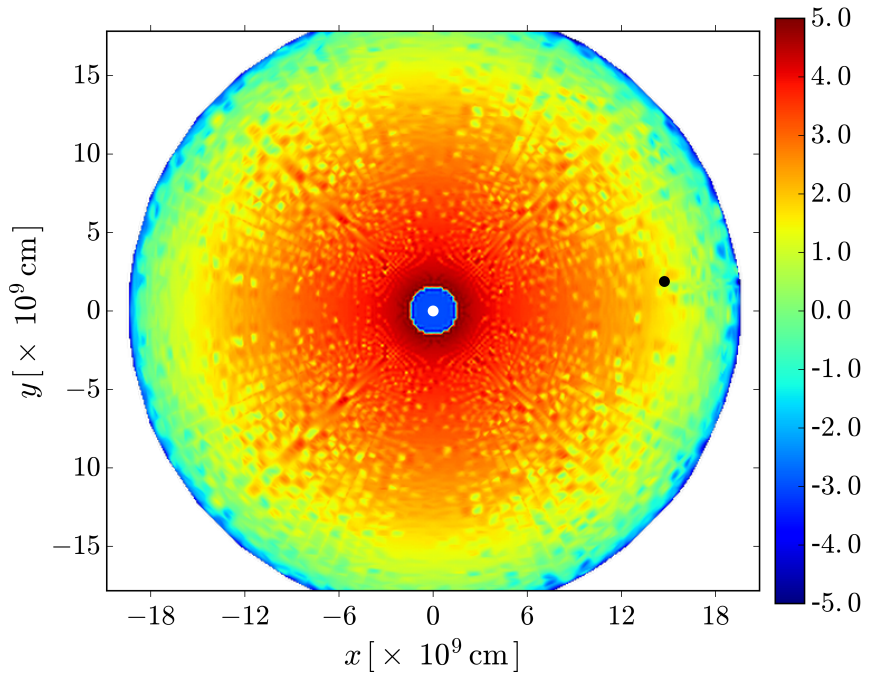
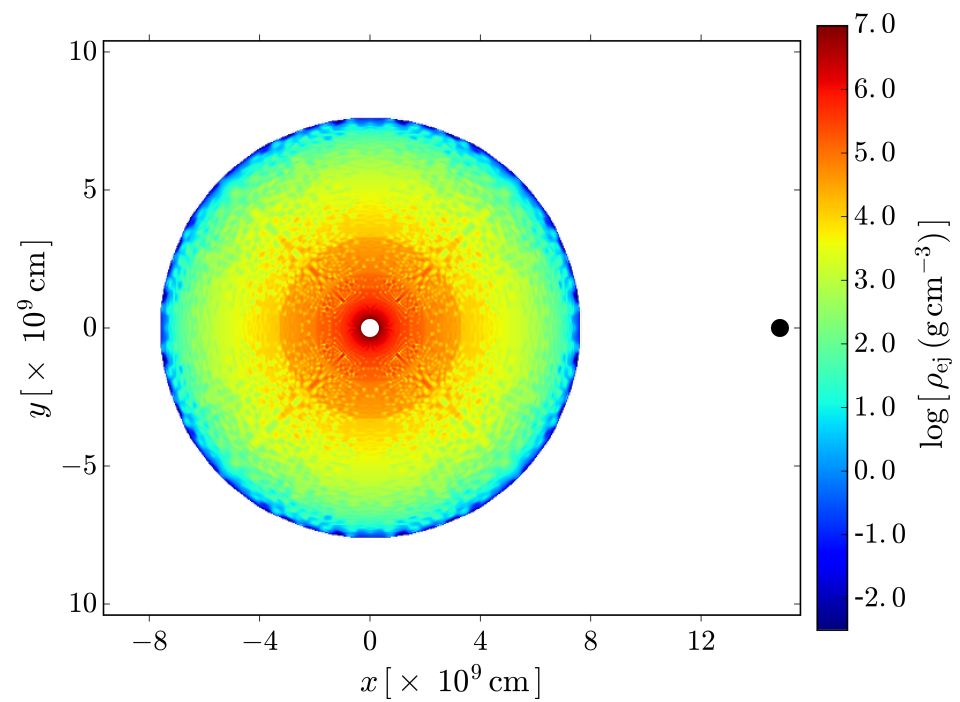
$$y^2 + z^2 = R_{\text{cap}}^2 = \left(\frac{2GM_{\text{NS}}}{v_{\text{rel}}^2(a, t)} \right)^2 (1 - 4\epsilon_v y)$$

IGC simulation

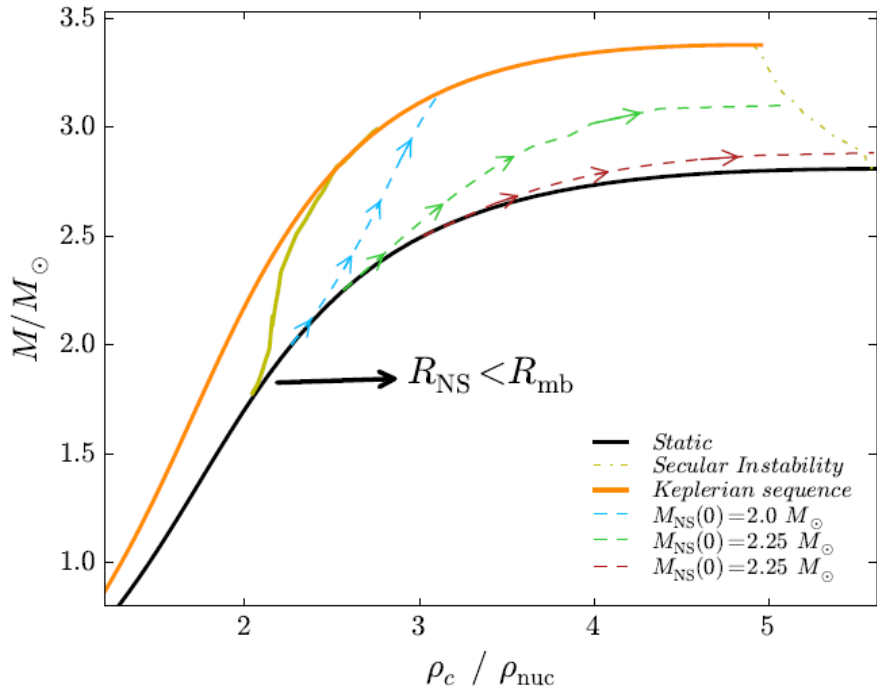
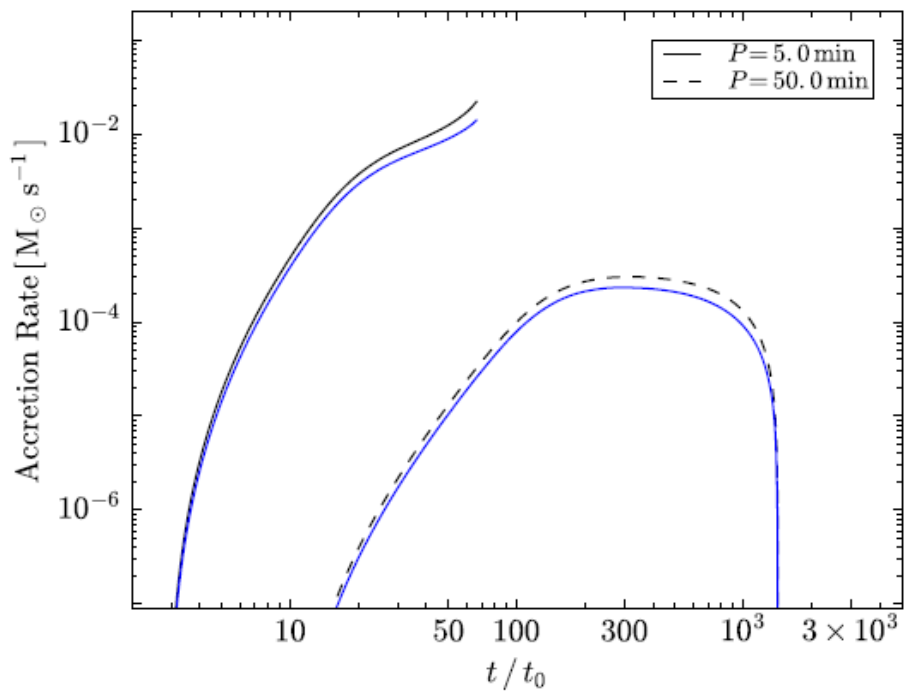
Becerra, Cipolletta, Fryer, Rueda, Ruffini,
ApJ 2015: arXiv:1505.07580



Visualizing the IGC process



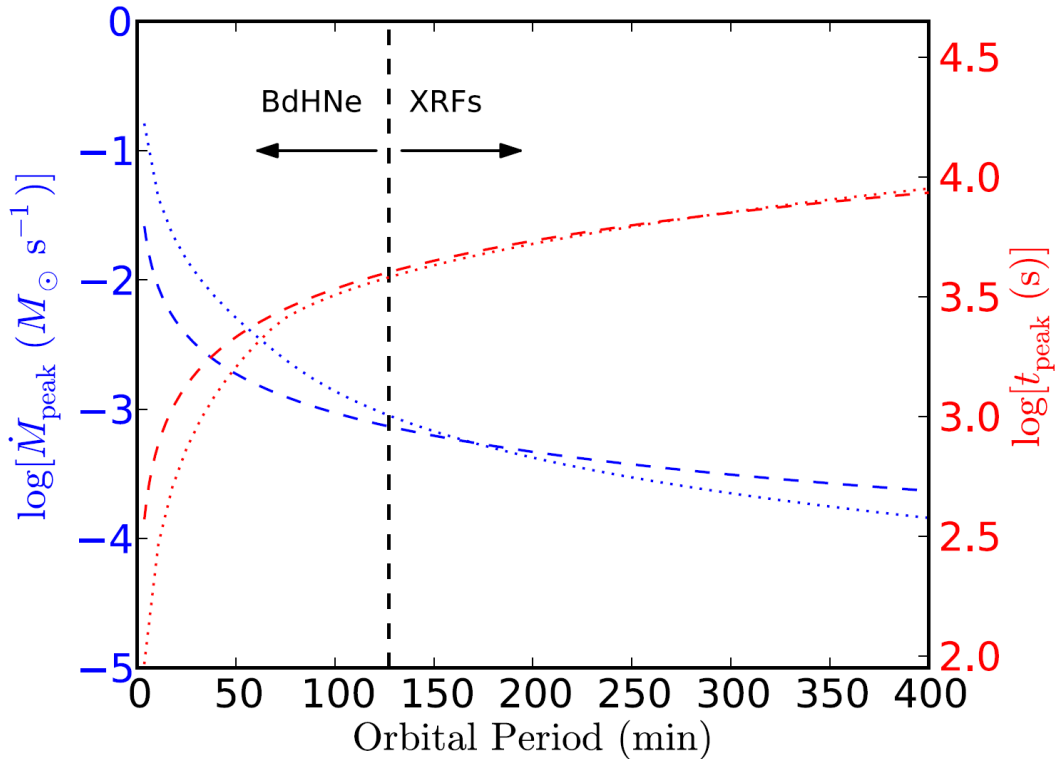
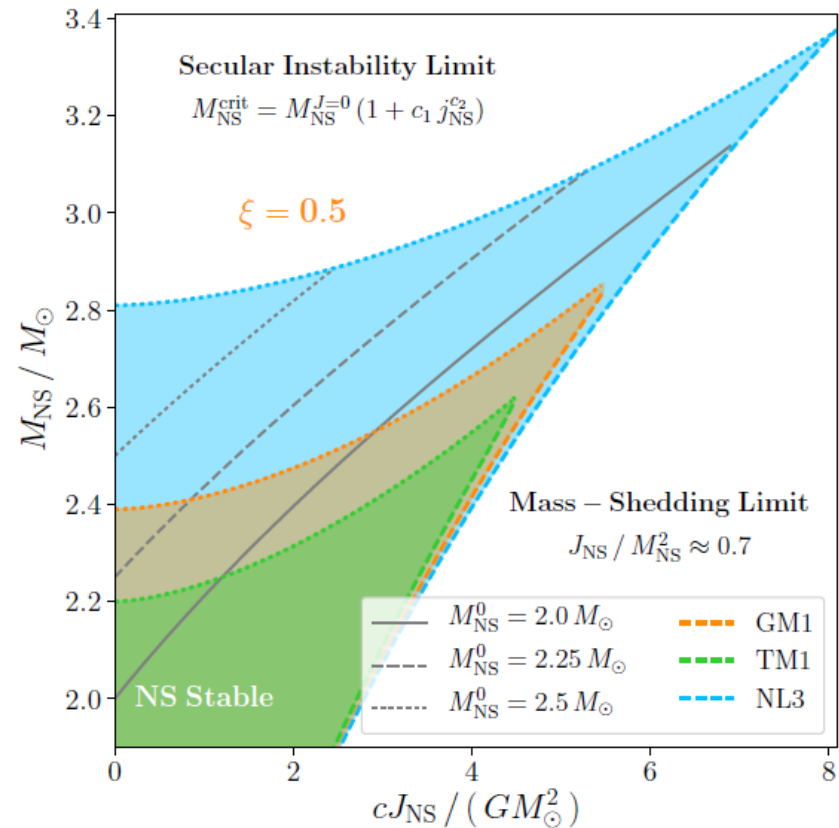
NS evolution up to the instability point



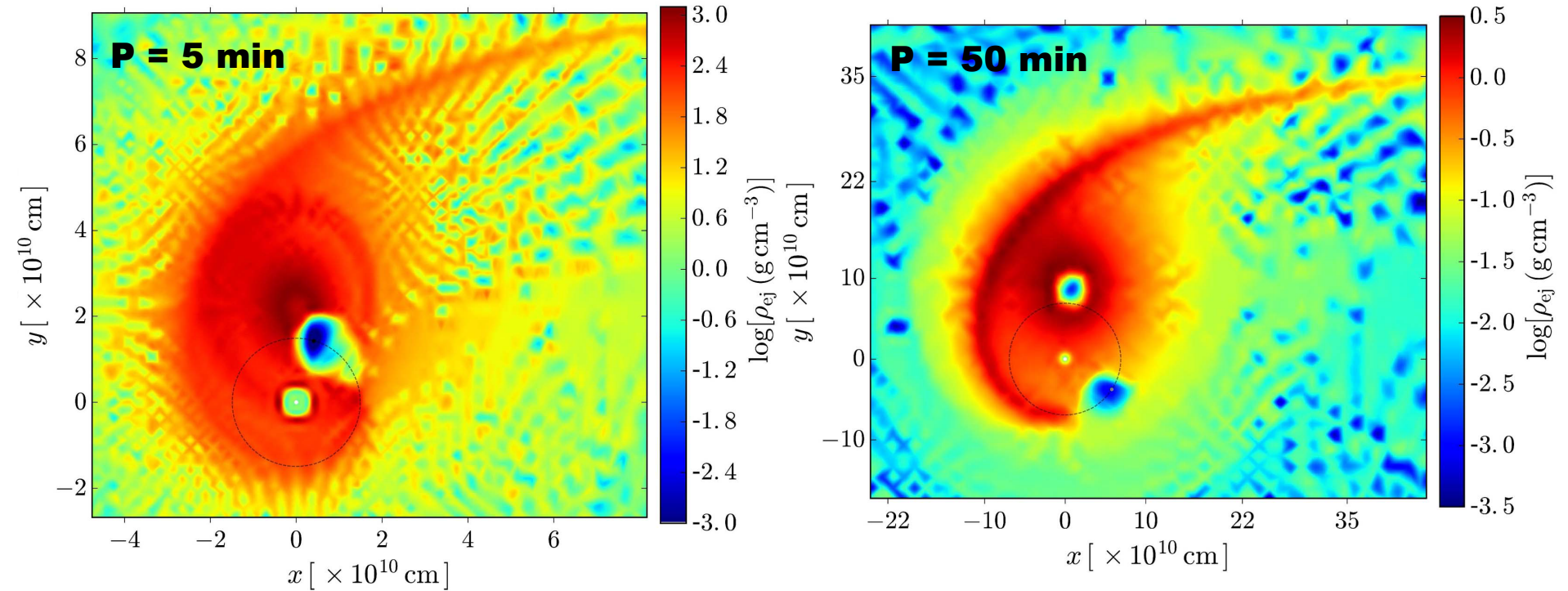
Becerra, Cipolletta, Fryer, Rueda, Ruffini, ApJ 2015; arXiv: 1505.07580
ApJ 2016; arXiv:1606.02523

X-ray Flashes - BdHNe Separatrix

(Becerra, Bianco, Fryer, Rueda, Ruffini, ApJ 2016; arXiv:1606.02523)

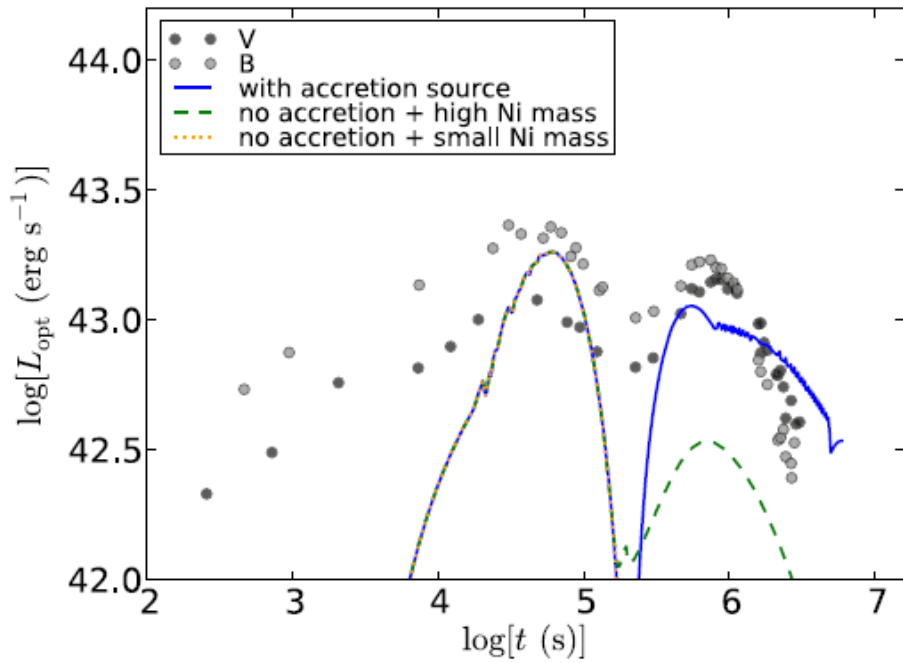
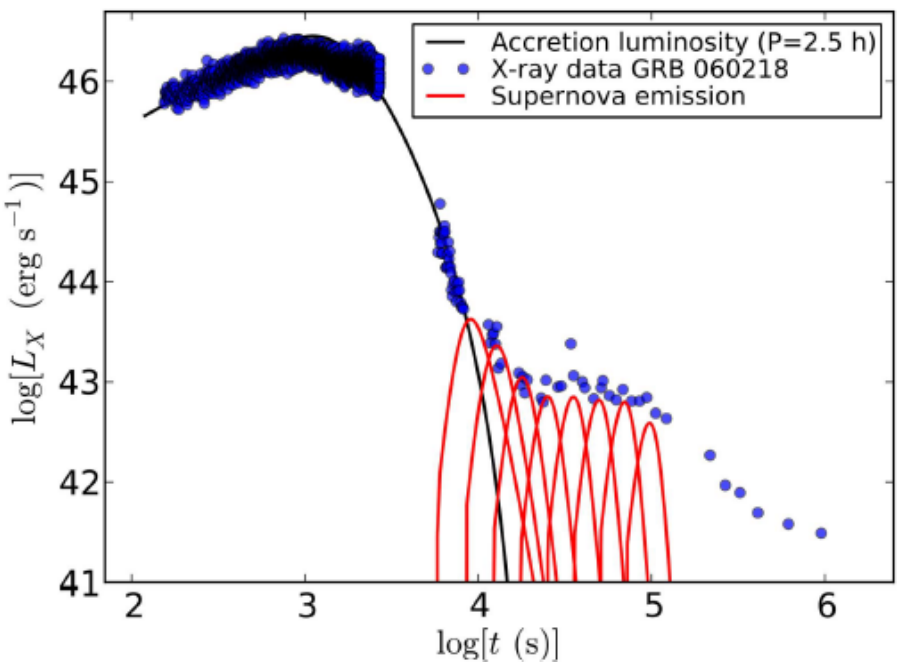


X-ray Flashes and BdHNe

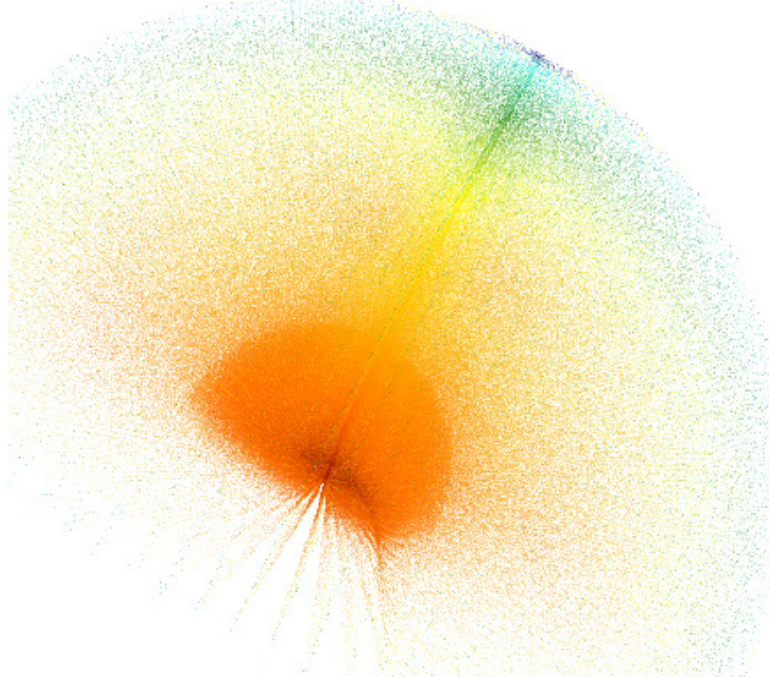
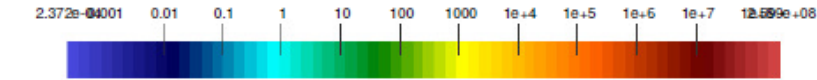
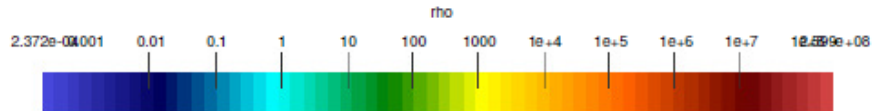
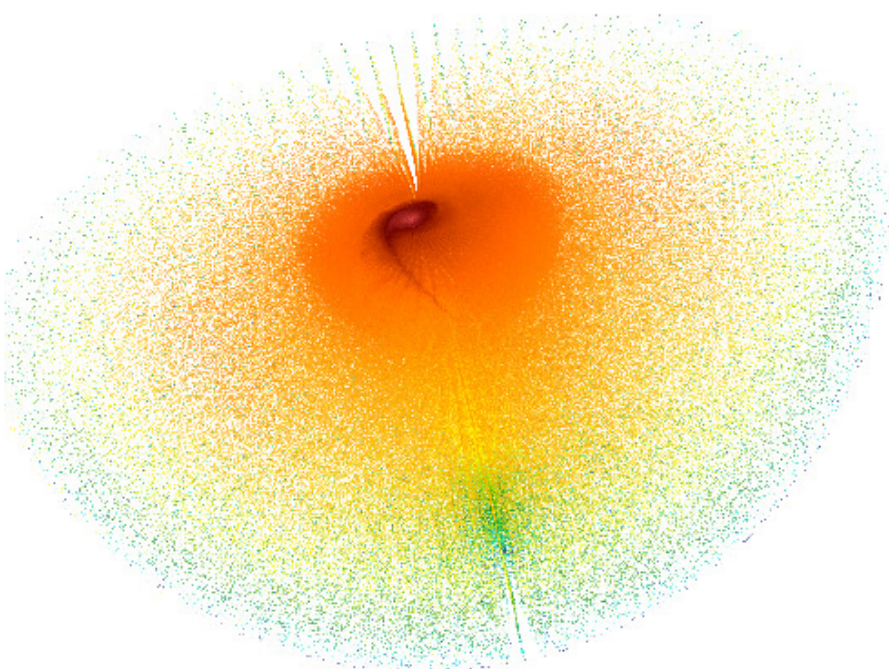


Becerra, Bianco, Fryer, Rueda, Ruffini, ApJ 2016;arXiv:1606.02523

An XRF example (GRB 060218): X-rays and optical emission



Ejecta density distribution at NS collapse instant



See R. Ruffini, R. Moradi and Yu Wang talks for consequences of the 3D structure

Latest simulations (SPH): ICRANet-LANL Collaboration

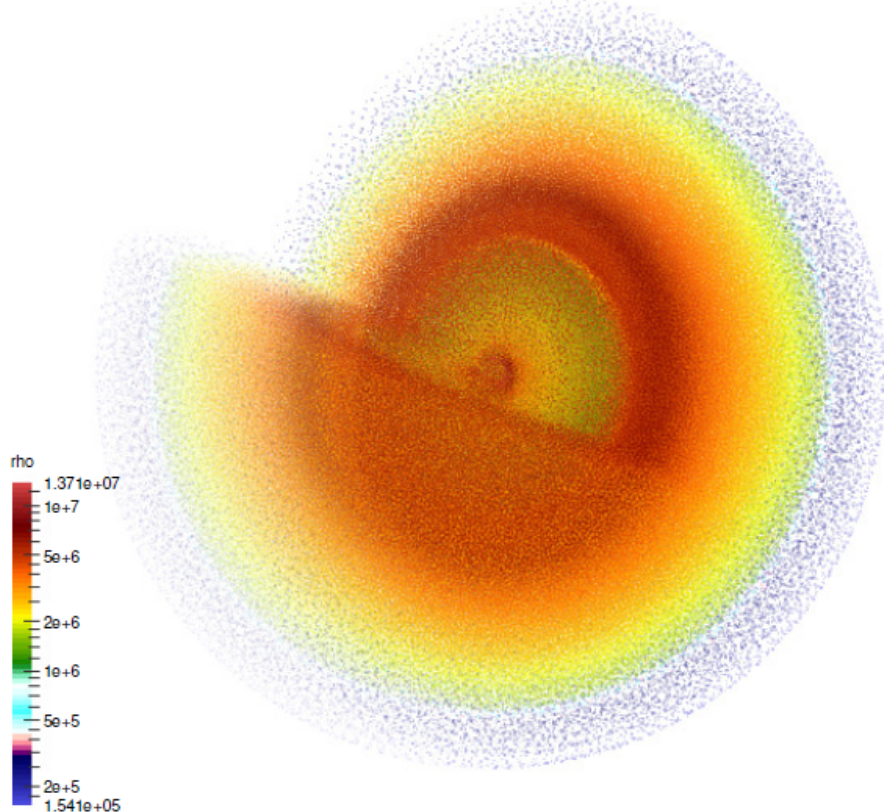
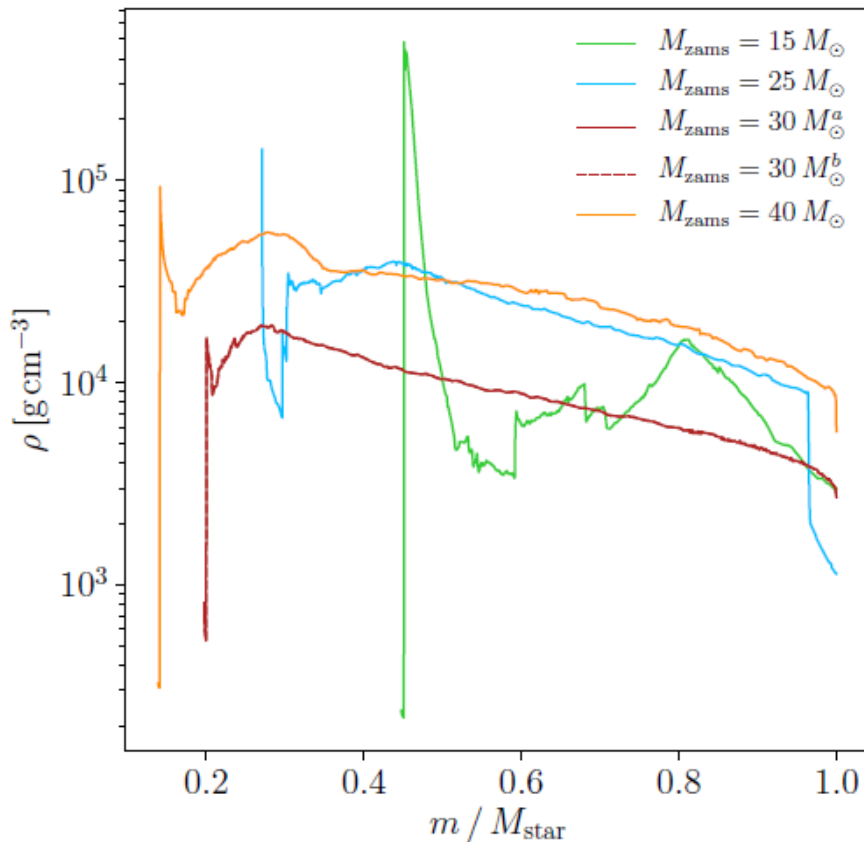
CO core-NS properties

M_{ZAMS} (M_{\odot})	M_{rem} (M_{\odot})	M_{ej} (M_{\odot})	R_{core} (10^8 cm)	R_{star} (10^9 cm)	V_{star} (10^8 cm/s)	E_{grav} (10^{51} erg)	m_j ($10^{-6} M_{\odot}$)
15	1.30	1.606	8.648	5.156	9.75	0.2149	$0.2 - 4.4$
25	1.85	4.995	2.141	5.855	5.43	1.5797	$2.2 - 11.4$
30^{a}	1.75	7.140	28.33	7.751	8.78	1.7916	$1.9 - 58.9$
30^{b}	1.75	7.140	13.84	7.830	5.21	1.5131	$1.9 - 58.9$
40	1.85	11.50	19.47	6.529	6.58	4.4305	$2.3 - 72.3$

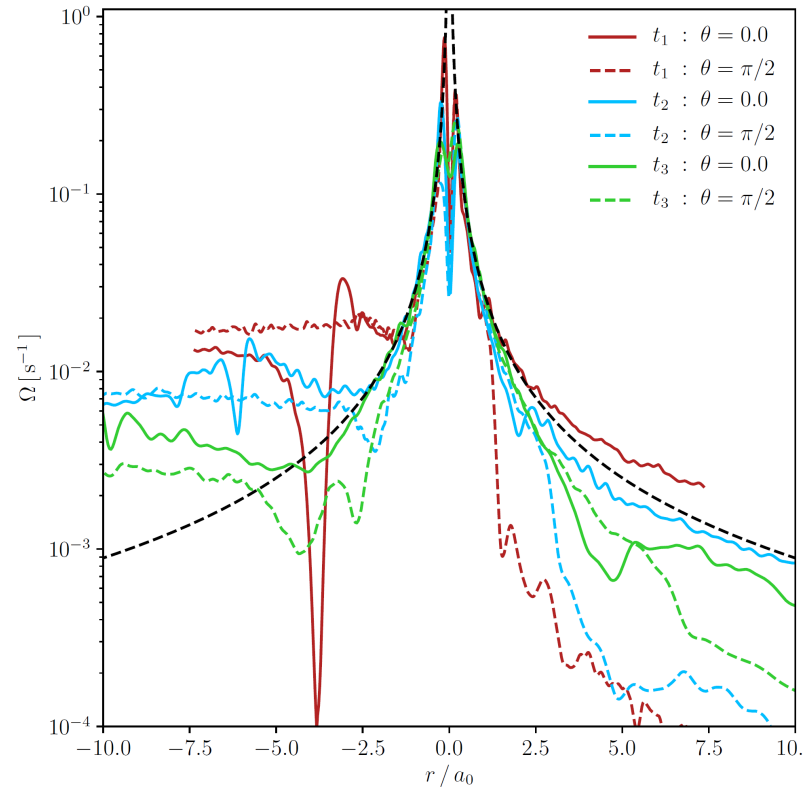
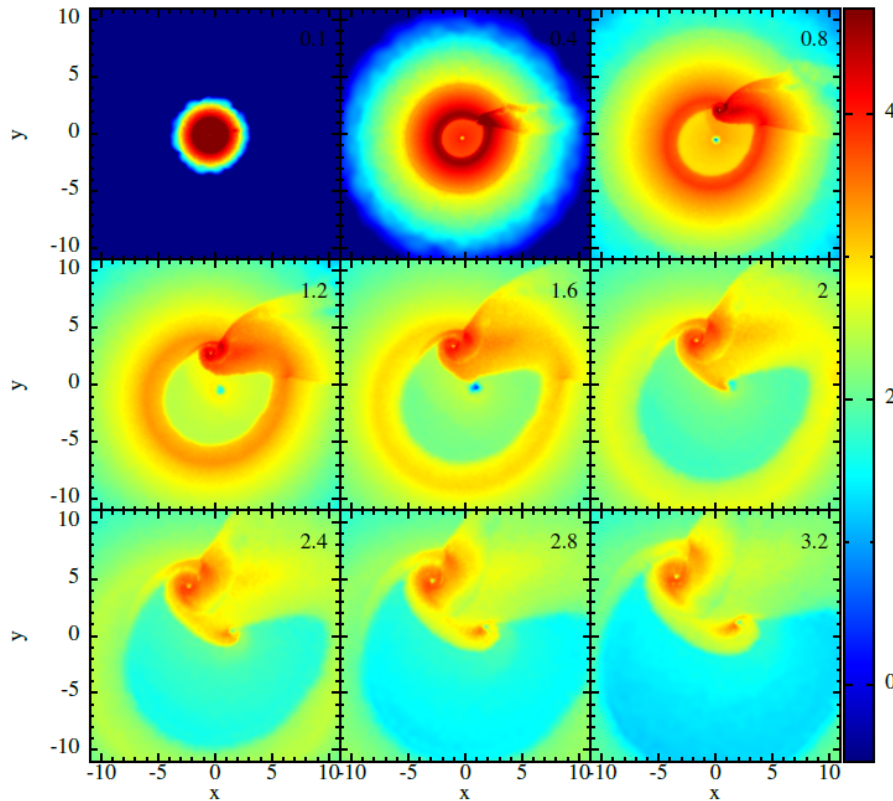
SPH Simulations I

CO-Core Progenitor: $25 M_{zams}$
 Total energy: $1.57 \times 10^{51} \text{ ergs}$
 Ejected Mass: $5.0 M_{\odot}$
 $\nu - NS$ Mass: $1.85 M_{\odot}$
 NS Mass: $2.0 M_{\odot}$
 Orbital Period : $\approx 5 \text{ minutes}$
 Orbital Separation: $1.35 \times 10^{10} \text{ cm}$

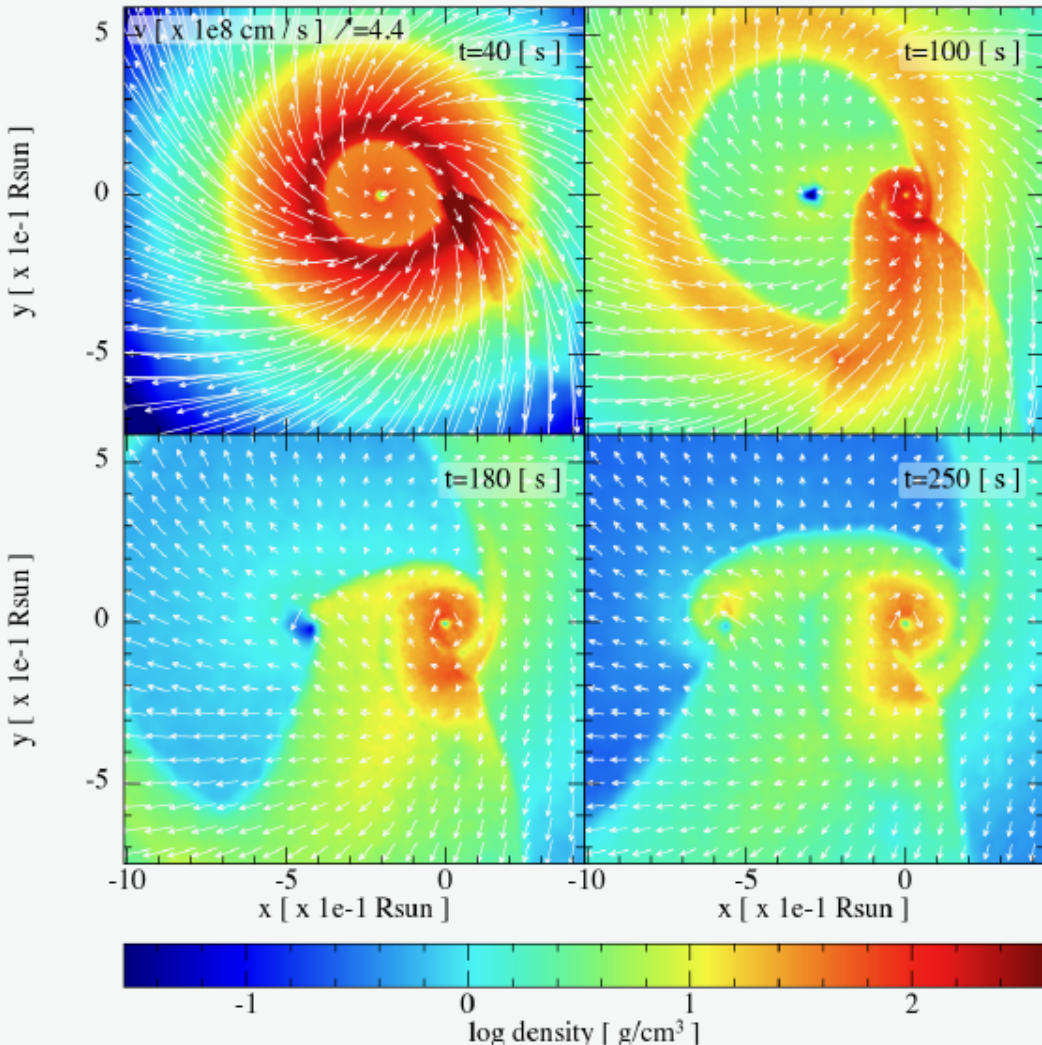
SN at t=0 (shock at CO-core surface)



BdHNe: orbital plane view

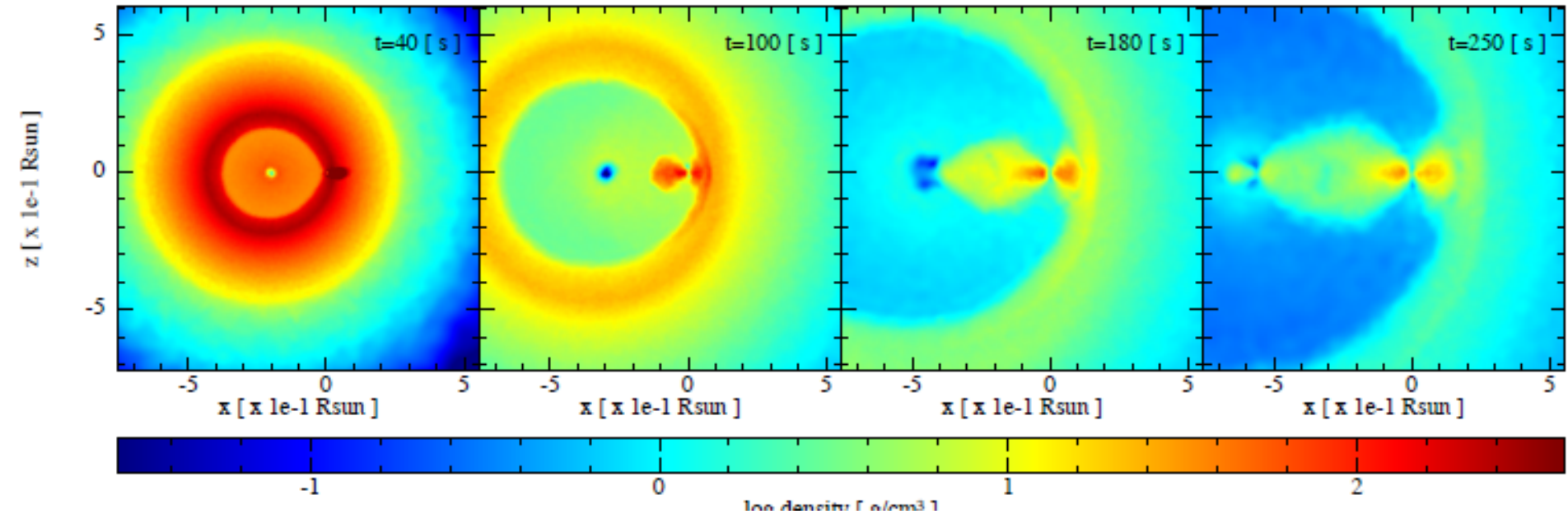


BdHN: orbital plane view

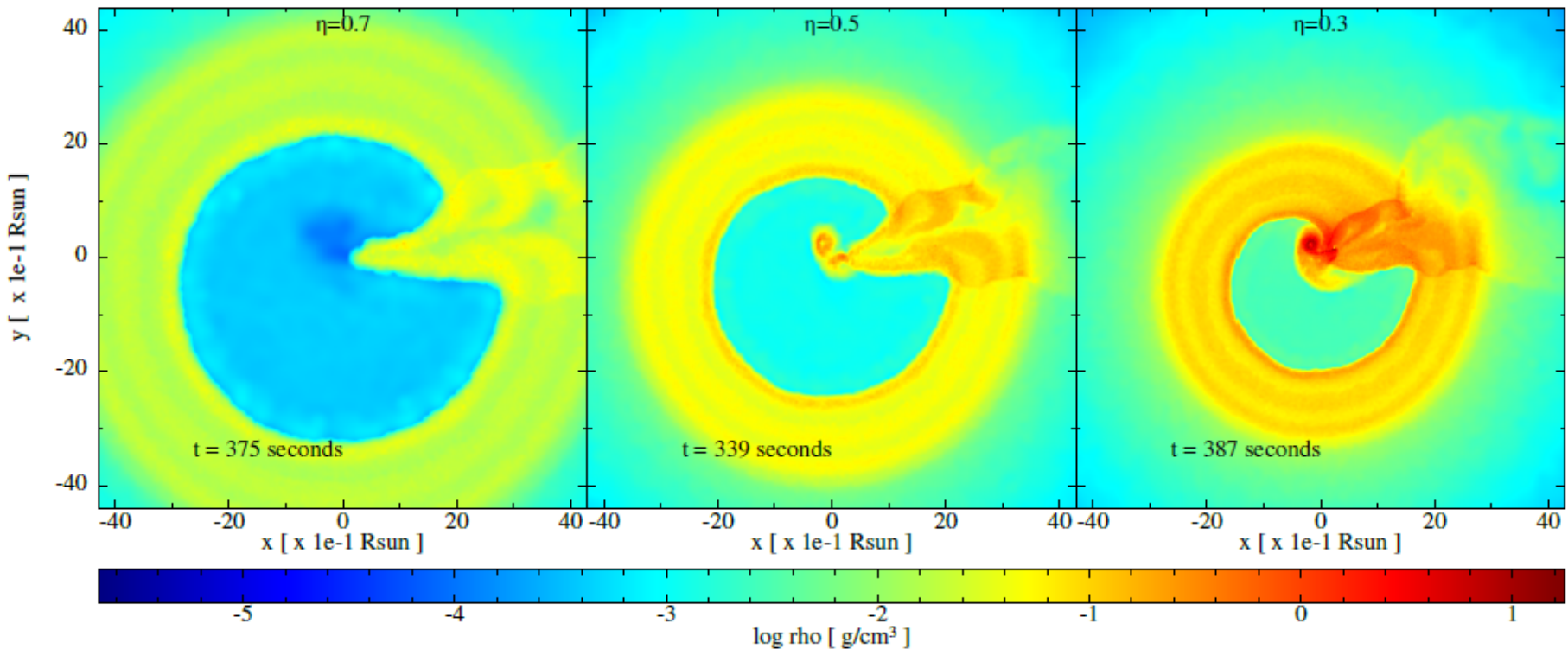


Becerra, Ellinger, Fryer,
Rueda, Ruffini;
arXiv:1803.04356

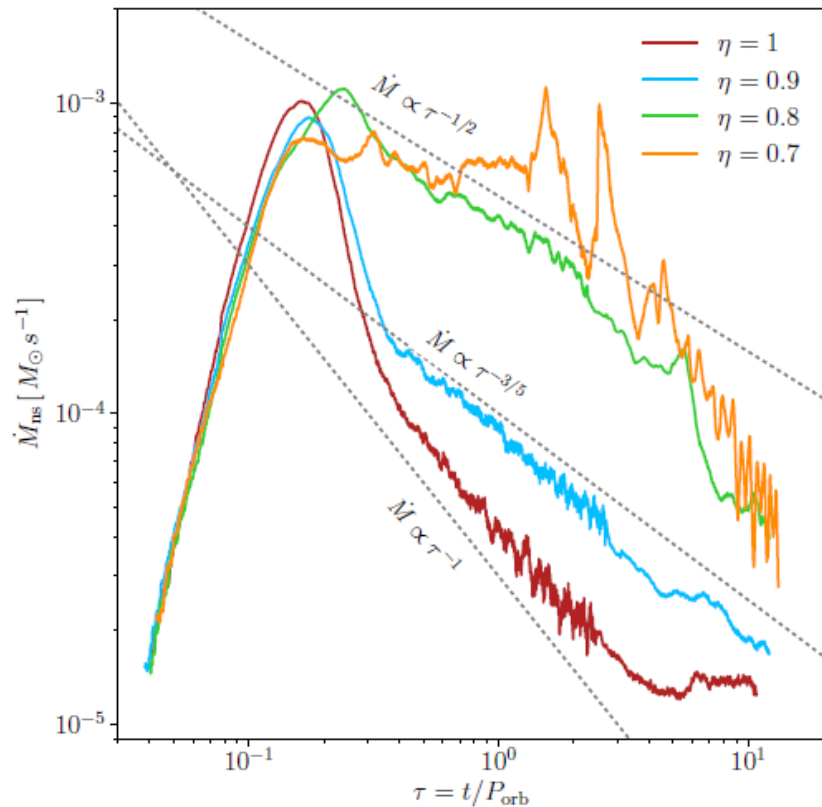
BdHNe: polar view and disk-like structure



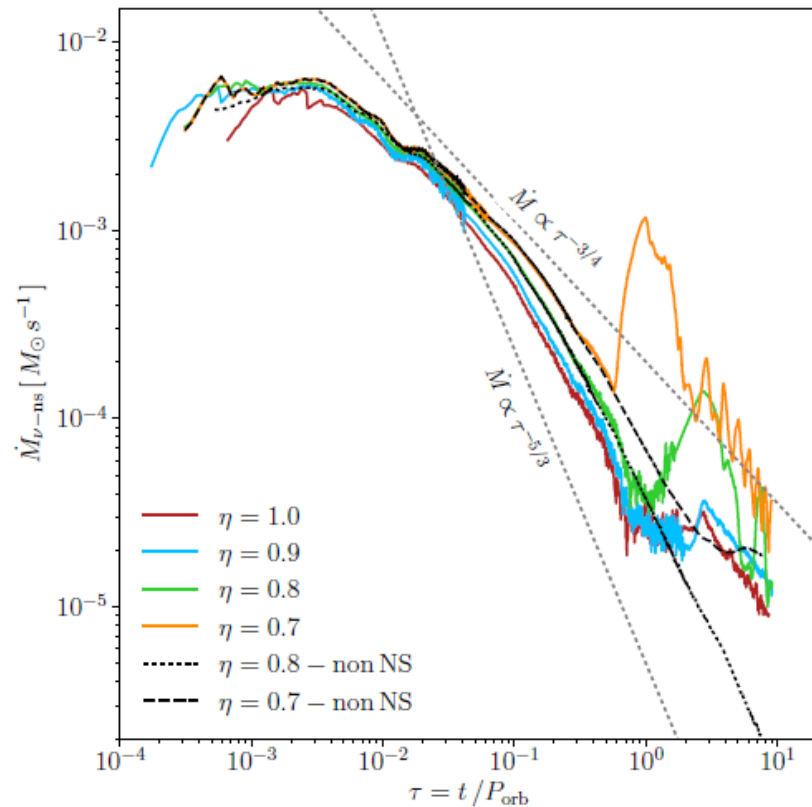
BdHNe and the orbital plane view: “fortune cookie” morphology



Accretion rate onto the NS and newNS

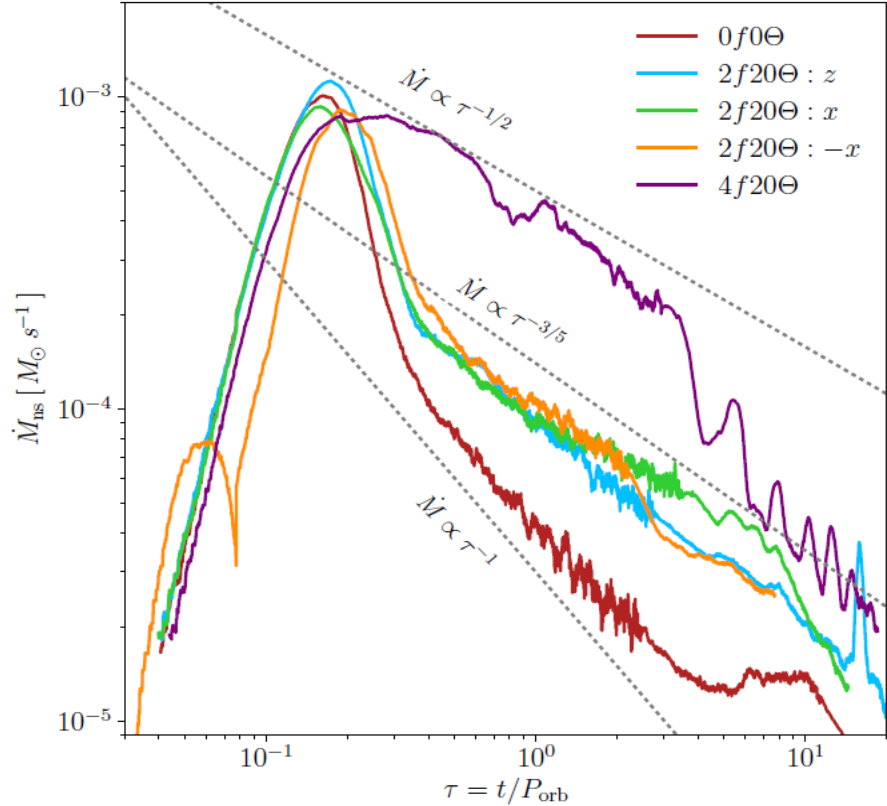
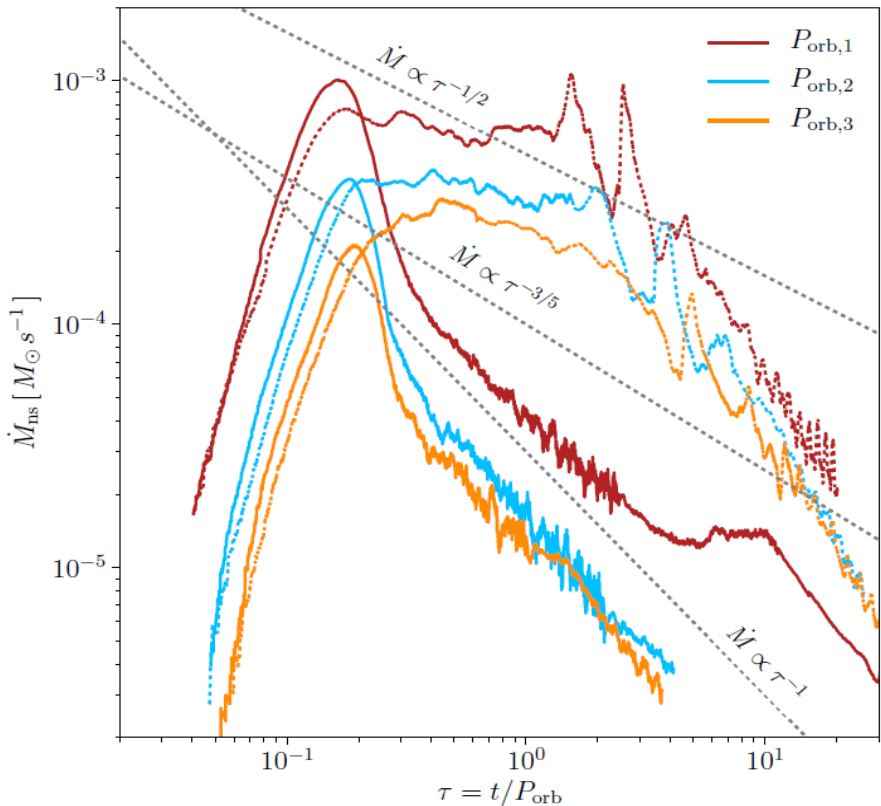


(a) NS star mass accretion rate

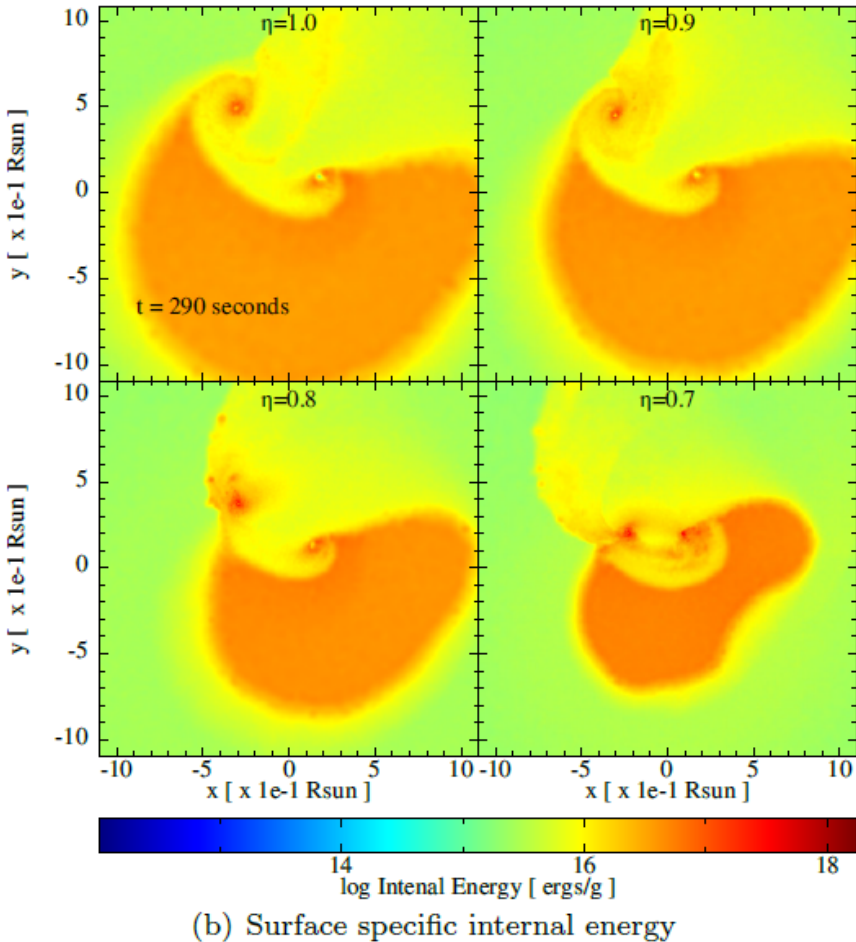
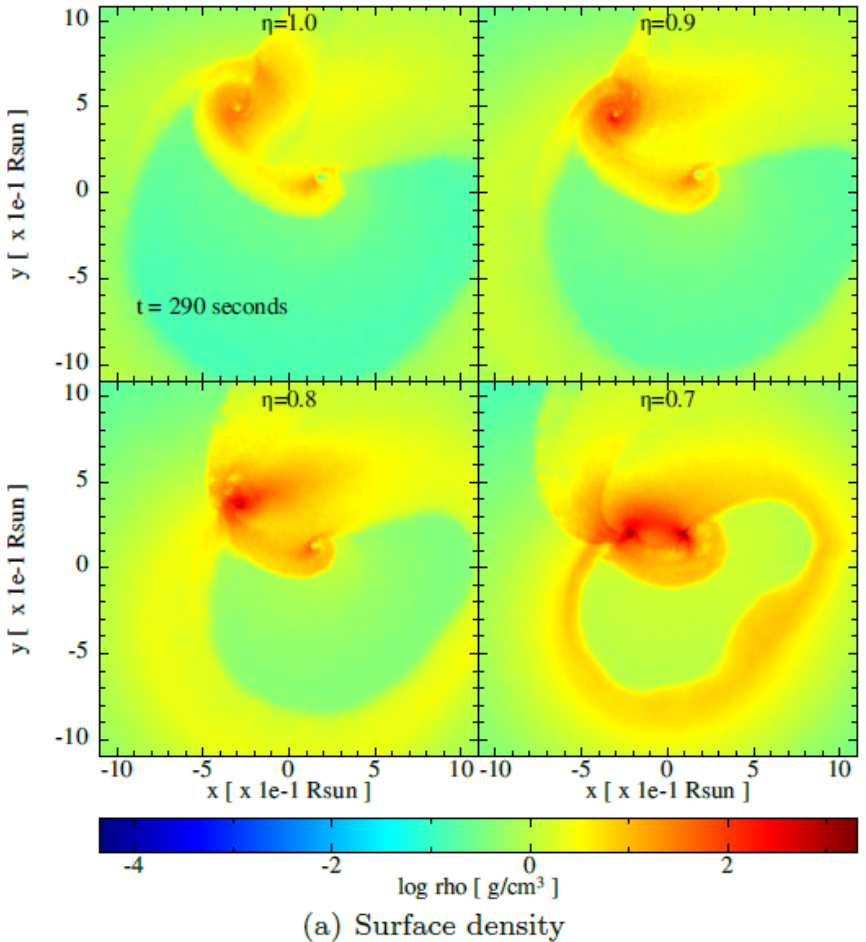


(b) ν NS mass accretion rate

Scaling with the orbital period and asymmetric explosion effects



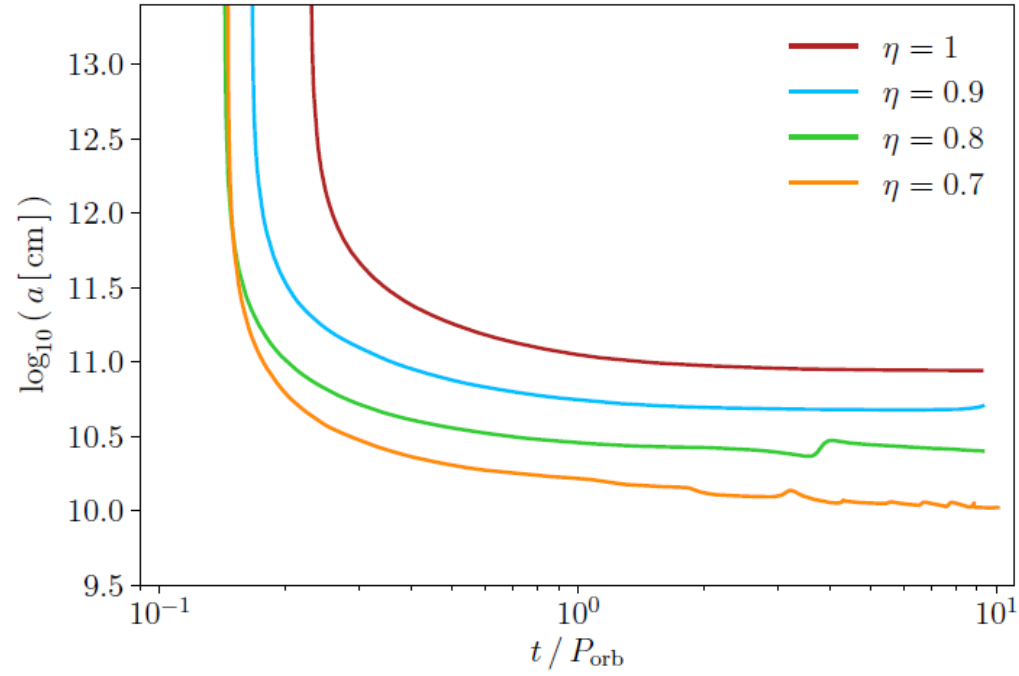
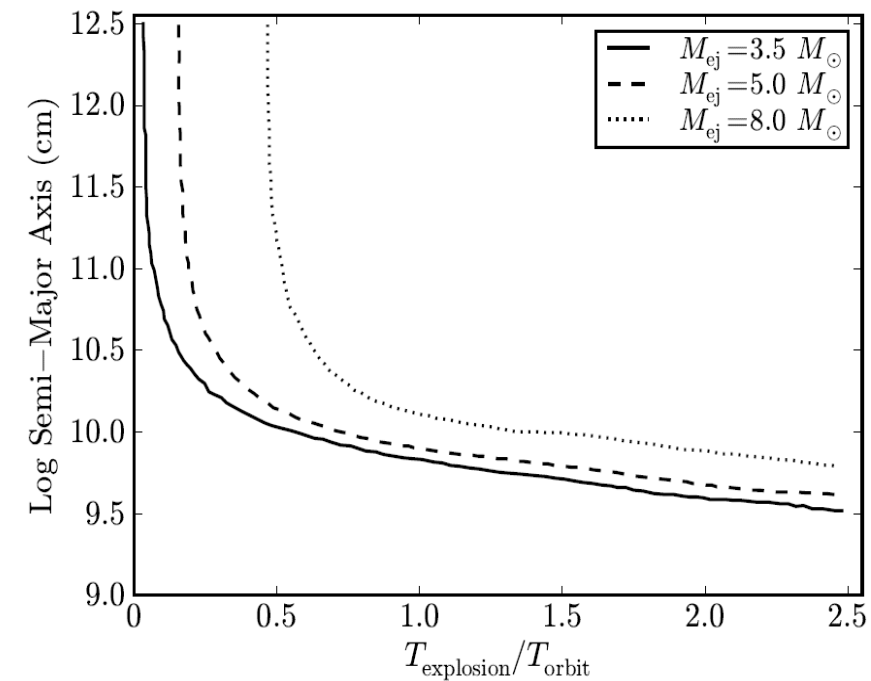
Orbital separation evolution



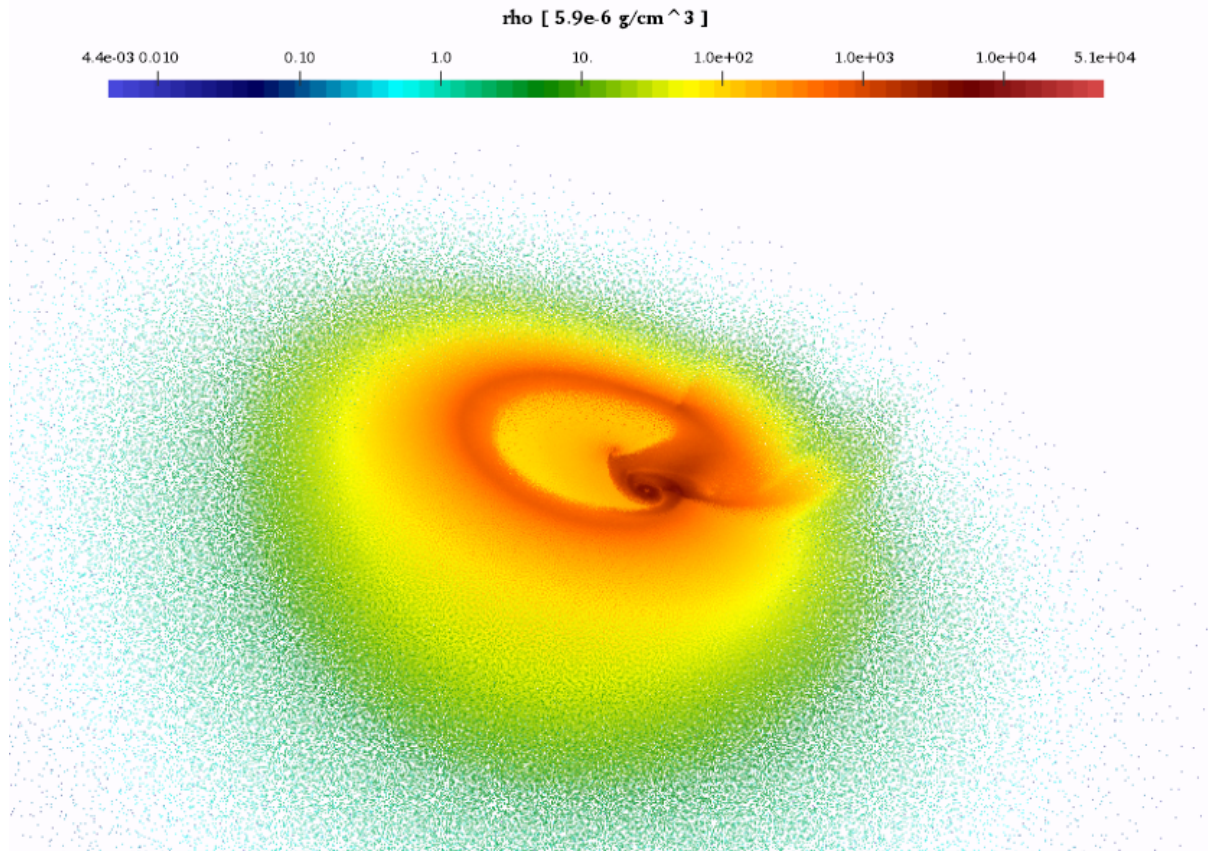
Some results of an specific simulation

Model	η	$E_k + U_i$ (10^{51} erg)	$P_{\text{orb},i}$ (s)	$a_{\text{orb},i}$ (10^{10} cm)	$m_{\nu\text{ns,fb}}$ (m_\odot)	V_{kick} (10^4 cm/s)	$m_{\nu\text{ns}}$ (m_\odot)	m_{ns} (m_\odot)	V_{CM} (10^7 cm/s)	$P_{\text{orb,f}}$ (s)	$a_{\text{orb,f}}$ (10^{10} cm)	e	m_{bound} (M_\odot)	bound	
$M_{\text{zams}} = 30 M_\odot$ Progenitor - exp 2															
30m1p1eb	1.0	3.26	363.8	1.667	4.184	141.30	3.675	2.382	3.59	727.929	2.209	0.5686	0.331	yes	
30m1p12eb	1.2	3.91	363.8	1.667	2.462	147.79	2.515	2.376	5.86	2764.53	5.0092	0.733	0.133	yes	
30m2p12eb	1.2	3.91	623.27	2.410	2.462	147.79	2.621	2.228	4.85	9425.47	11.3017	0.848	0.029	yes	
30m1p2eb	2.0	6.45	363.8	1.667	1.771	13.89	1.783	2.077	9.50	—	—	1.447	5.7×10^{-3}	no	
30m1p31eb	3.14	10.02	363.8	1.667	1.766	5.21	1.768	2.017	9.95	—	—	1.712	6.5×10^{-4}	no	
νNS															
NS															
		$\chi = 0.5$			$\chi = 1.0$						$\chi = 0.5$			$\chi = 1.0$	
CO _{core}	Model	L_{tot}	$M_{\nu\text{NS}}$	$j_{\nu\text{NS}}$	Fate	$M_{\nu\text{NS}}$	$j_{\nu\text{NS}}$	Fate	L_{tot}	M_{NS}	j_{NS}	Fate	M_{NS}	j_{NS}	Fate
M_{zams}		$c/(GM_\odot^2)$	M_\odot	$c/(GM_\odot^2)$		M_\odot	$c/(GM_\odot^2)$		$c/(GM_\odot^2)$	M_\odot	$c/(GM_\odot^2)$		M_\odot	$c/(GM_\odot^2)$	
$30 M_\odot$ ^b															
30m1p1eb		64.935	2.379	2.614	Sc-in	2.215	3.507	M-sh	19.995	2.244	1.099	Sc-in	2.307	2.634	Stb
30m1p12eb		28.432	2.362	2.541	Stb	2.200	3.392	M-sh	33.681	2.244	1.100	Sc-in	2.304	2.606	Stb
30m2p12eb		26.508	2.397	2.807	Sc-in	2.162	3.297	M-sh	23.922	2.1801	0.802	Stb	2.1827	1.572	Stb
30m1p2eb		2.819	1.777	0.106	Stb	1.777	0.196	Stb	7.846	2.061	0.271	Stb	2.061	0.546	Stb
30m1p31eb		0.721	1.766	0.0611	Stb	1.766	0.105	Stb	1.6715	2.014	0.062	Stb	2.014	0.122	Stb

NS-BH binaries produced by BdHNe

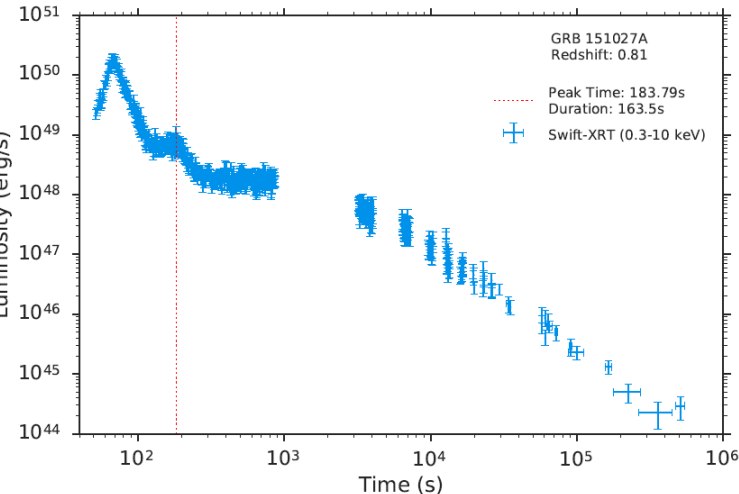
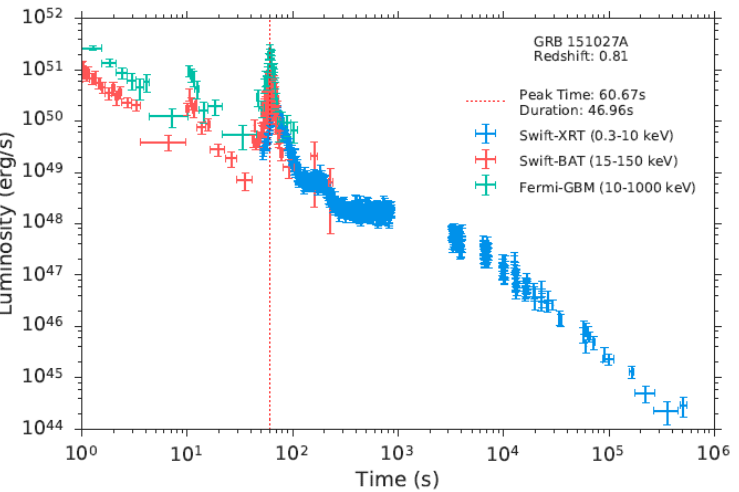
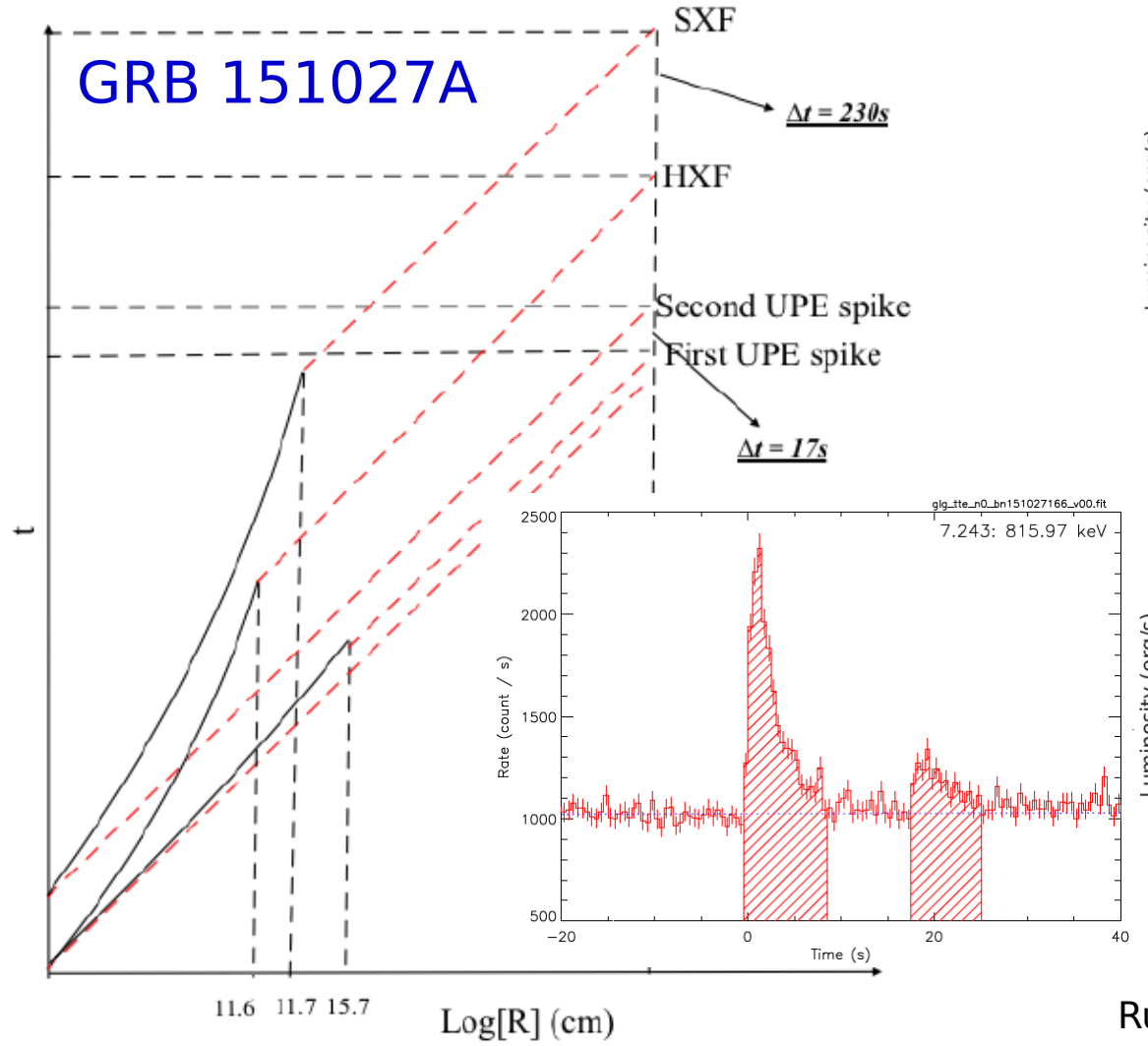


3D view of a BdHN



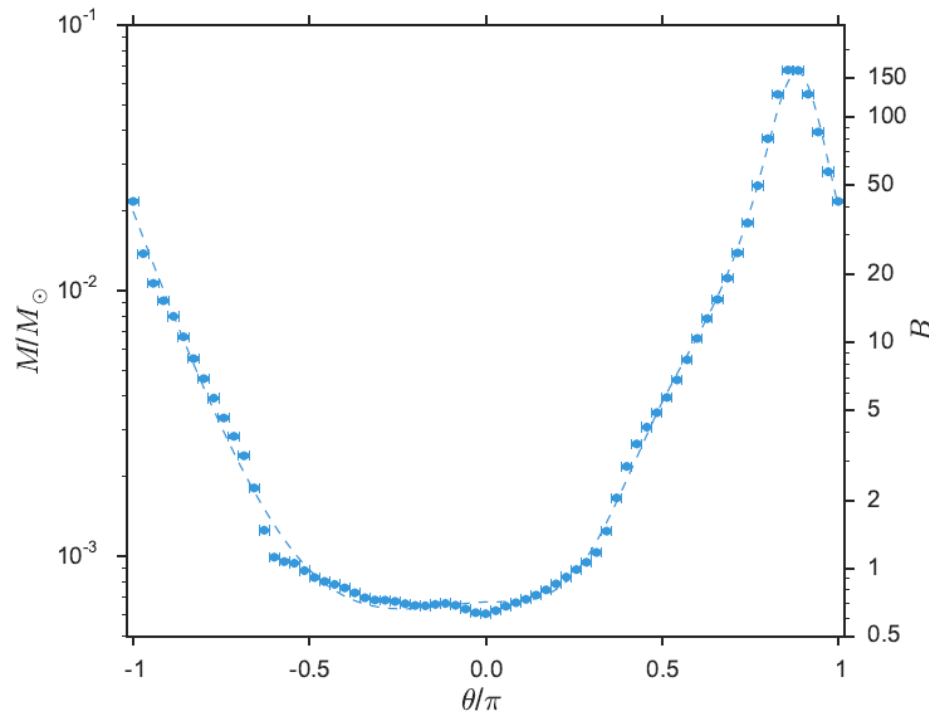
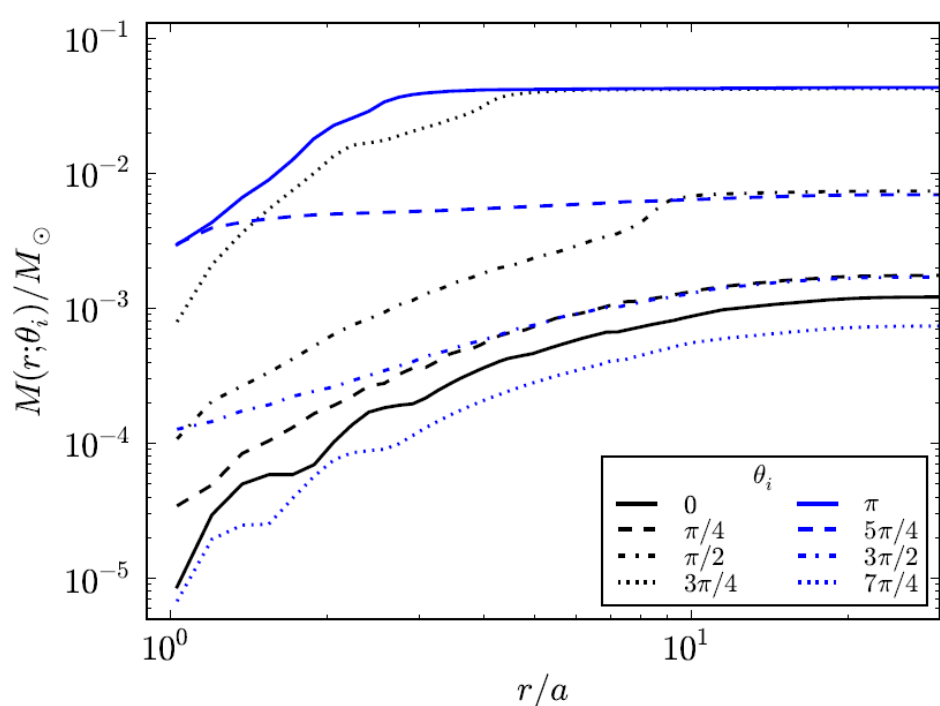
See R. Ruffini, R. Moradi and Yu Wang talks for consequences of the 3D structure

GRB 151027A



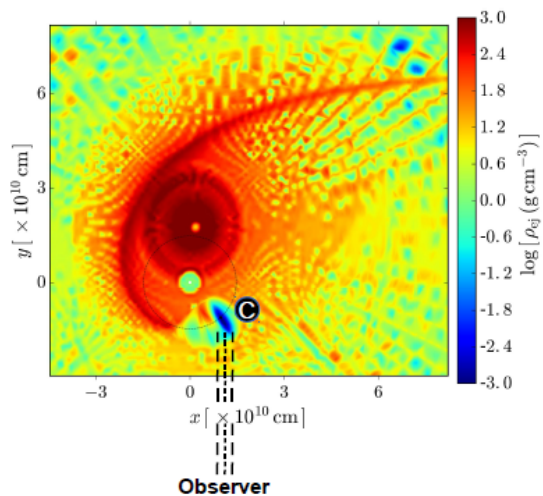
Baryon load on the orbital plane

R. Ruffini, L. Becerra, C. L. Bianco, et al.; arXiv:1712.05001; Ruffini et al. ApJ 852, 53 (2018)

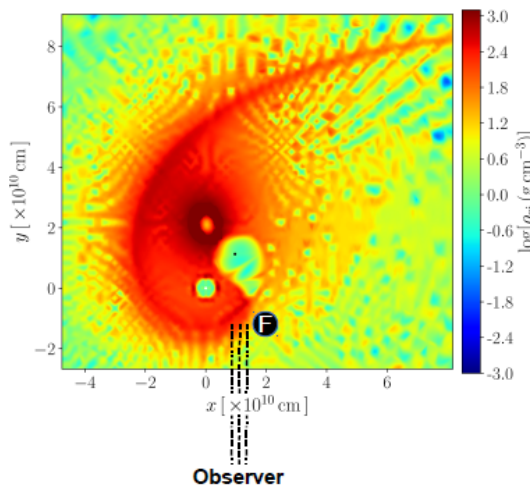


Baryon load parameter = B = plasma energy / baryon target mass-energy

(a)

 $t = 0 \text{ s}$ 

(b)

 $t = 56.7 \text{ s}$ 

(c)

 $t = 236.8 \text{ s}$ 